An intense terminal epoch of widespread fluvial activity on early Mars: 1. Valley network incision and associated deposits

Alan D. Howard
Department of Environmental Sciences, University of Virginia, Charlottesville, Virginia, USA

Jeffrey M. Moore
NASA Ames Research Center, Moffett Field, California, USA

Rossman P. Irwin III
Center for Earth and Planetary Studies, National Air and Space Museum, Smithsonian Institution, Washington, D. C., USA

Received 15 April 2005; revised 26 July 2005; accepted 8 August 2005; published 4 November 2005.

[1] We present evidence that a final epoch of widespread fluvial erosion and deposition in the cratered highlands during the latest Noachian or early to mid-Hesperian was characterized by integration of flow within drainage networks as long as 4000 km and trunk valley incision of 50 to 350 m into earlier Noachian depositional basins. Locally deltaic sediments were deposited where incised valley systems debouched into basins. Large alluvial fans of sediment deposited from erosion of alcoves in steep crater walls probably formed contemporaneously. The depth of incision below Noachian surfaces correlates strongly with the gradient and the total valley length, suggesting consistent regional hydrology. Estimated discharges from channel dimensions indicate flow rates equivalent to mean annual floods in terrestrial drainage basins of equivalent size. Such high flow rates imply either runoff directly from precipitation or rapid melting of accumulated snow. Development of duricrusts on the Noachian landscape may have contributed to focusing of late-stage erosion within major trunk drainages. This late-stage epoch of intense fluvial activity appears to be fundamentally different than the fluvial environment prevailing during most of the Noachian Period, which was characterized by widespread fluvial erosion of highlands and crater rims, deeply infilling crater floors, and intercrater basins through ephemeral fluvial activity, and development of local rather than regionally integrated drainage networks.

Citation: Howard, A. D., J. M. Moore, and R. P. Irwin III (2005), An intense terminal epoch of widespread fluvial activity on early Mars: 1. Valley network incision and associated deposits, *J. Geophys. Res.*, *110*, E12S14, doi:10.1029/2005JE002459.

1. Introduction

[2] The highlands of Mars record extensive fluvial erosion that occurred during the Noachian Period, extending from the earliest observable features until the Hesperian at about 3.5 Ga B.P. [*Hartmann*, 2005]. Considerable debate has occurred since the first global observations of Mars by Mariner 9 (1971–2) about the source of runoff and the total erosion required to produce the widespread valley networks. Global topographic mapping by the Mars Orbiter Laser Altimeter (MOLA) (1997–2001) has revealed that fluvial erosion may have stripped several hundred meters of surface materials on the observable landscape and infilled crater floors [*Hynek and Phillips*, 2001; *Craddock and Howard*, 2002]. This extensive fluvial redistribution of sediment has led to an emerging consensus that a hydrologic cycle consisting of precipitation and runoff was required during the Noachian [*Grant*, 2000; *Hynek and Phillips*, 2001, 2003; *Craddock and Howard*, 2002; *Irwin and Howard*, 2002; *Forsberg-Taylor et al.*, 2004].

[3] Following the Noachian, the climate changed due to a reduction of atmospheric temperature and pressure, which resulted from loss of atmospheric components to space and through weathering reactions [*Fanale et al.*, 1992; *Carr*, 1999]. This reduction in mass diminished the capability of the atmosphere to support a precipitation-based hydrologic cycle, and some of the early water inventory was incorporated into a cryosphere and polar deposits [*Clifford*, 1993; *Carr*, 1996; *Clifford and Parker*, 2001]. During the Hesperian and Amazonian time periods fluvial activity was primarily limited to formation of outflow channels, primarily thought to result from local melting of the cryosphere by volcanic processes or impacts [*Carr*, 1979, 1996; *Clifford*, 1993; *Tanaka*, 1999; *Clifford and Parker*, 2001]. However, valley net-

0148-0227/05/2005JE002459$09.00

works of Hesperian and Amazonian age have been found, located primarily on the slopes of volcanoes or within the Tharsis volcanic province [*Gulick and Baker*, 1989; *Scott*, 1995]. These have usually been attributed to hydrothermal pumping of groundwater or to local precipitation from condensation of volcanic venting [*Gulick and Baker*, 1990; *Gulick*, 1998, 2001; *Dohm and Tanaka*, 1999], although recent high-resolution Thermal Emission Imaging System (THEMIS) images have revealed integrated drainage networks elsewhere in the Tharsis region of possibly late Hesperian age that are attributed to precipitation [*Mangold et al.*, 2004]. Fluvial erosion on the equatorial highlands since the Hesperian has apparently been restricted to small gullies on steep slopes [*Malin and Edgett*, 2000a], although outflow channel activity has continued through the Amazonian [*Mouginis-Mark*, 1990; *Burr et al.*, 2002].

[4] The apparent decline in widespread fluvial activity across much of Mars associated with rapid loss of surface atmospheric volatiles has resulted in a paradigm of gradually declining fluvial activity through the Noachian into the Hesperian Periods, with only localized erosion during the Hesperian [*Tanaka*, 1986; *Carr*, 1996]. Alternatively, *Grant and Schultz* [1990] suggest that erosion and deposition was episodic during the Noachian. It has also been suggested that this decline in activity was associated with a change in location and formative process of fluvial erosion. On the basis of Viking images, *Baker and Partridge* [1986] distinguished between older ''degraded'' valley networks on the Martian highlands, eroded by precipitation runoff, and younger ''pristine'' reaches restricted to downstream portions of the networks, which were eroded by groundwater sapping. This evolution from runoff to sapping has also been proposed by *Harrison and Grimm* [2005].

[5] In this paper we present observations from recent high-resolution images from the Mars Orbiter Narrow Angle Camera (MOC NA) and the THEMIS visual (VIS) and infrared wavelength (IR) cameras that indicate that a distinctive style of fluvial erosion and deposition occurred at a time period near the Noachian-Hesperian boundary. We term this ''late-stage'' fluvial activity in this paper. In accord with the observations of *Baker and Partridge* [1986] we find deep, late-stage incision of high-order (downstream) segments of valley networks in the equatorial regions of Mars. In addition, local occurrences of large alluvial fans and fluvial deltas record a period of deposition by sustained fluvial flows that appear to have had both an abrupt onset and cessation. Erosion earlier in the Noachian, although extensive, apparently was not conducive to deep channel incision or to formation of large alluvial fans and deltas. We suggest that these observations are consonant with a period of intense fluvial activity in the highlands of Mars lasting at least a millennium. We begin with a short review of the erosional process and landforms of the Noachian to contrast with those of the Noachian-Hesperian transition. We limit our discussion to the equatorial regions (latitude range $\pm 30^{\circ}$) because strong mantling and post-Noachian ice-related processes at more polar latitudes complicate landform analysis [e.g., *Soderblom et al.*, 1973; *Head et al.*, 2003]. A companion paper [*Irwin et al.*, 2005b] focuses on lacustrine and deltaic features of equivalent age and the relationship of late-stage fluvial activity to the evolution of the highlands-lowlands boundary.

2. Noachian Fluvial Processes

[6] MOC, THEMIS, and MOLA data support suggestions that extensive fluvial erosion and deposition occurred throughout the highlands during the Noachian [e.g., *Craddock and Maxwell*, 1993; *Craddock et al.*, 1997; *Grant*, 2000; *Hynek and Phillips*, 2001, 2003; *Craddock and Howard*, 2002; *Grant and Parker*, 2002; *Irwin and Howard*, 2002]. Sediment yields were high, infilling >10 km diameter craters with several hundred meters of sediment and creating alluvial ramps at the foot of highland relief, thus implying active chemical or physical weathering [*Craddock and Howard*, 2002; *Forsberg-Taylor et al.*, 2004]. Erosion of massifs and inner and outer crater wall slopes reached close to divides, and drainage densities locally approached terrestrial values [e.g., *Irwin and Howard*, 2002; *Hynek and Phillips*, 2003; *Stepinski and Collier*, 2004]. Integrated drainage networks hundreds of kilometers long were formed where regional slopes existed. Erosion of the highlands may have averaged several hundred meters, although rates should have varied with regional slope and local climate. Estimates derived from depth of incision or basin infilling are probably conservative because frequent impact cratering reset the topography and disrupted drainage networks [*Irwin and Howard*, 2002]. Both during and subsequent to their formation these fluvial features were highly degraded by impacts, eolian transport, mass wasting and in many areas by extensive airfall mantling by dust, large-impact ejecta, or volcanic ash [e.g., *Grant and Schultz*, 1990; *Moore*, 1990; *Malin and Edgett*, 2000b; *Arvidson et al.*, 2003]. The statistics of degraded crater infilling and crater counts in the highlands are consistent with degradation primarily by fluvial processes at a rate that was proportional to the rate of new impacts, implying a gradual decline in fluvial activity accompanying the gradual decline in impact rate [*Forsberg-Taylor et al.*, 2004].

[7] The environment that supported such intensive erosion during the Noachian is controversial, but the prevailing interpretation is that widespread, although episodic, precipitation (as snow or rain) occurred with associated (melt) runoff and groundwater seepage. The abundance of alluvial plains at the base of crater walls and the small number of breached crater rims suggests an arid climate, with ephemeral lakes in the larger craters. Overall, however, long-term erosion rates during the mid to late Noachian were slow, being comparable to terrestrial hyperarid deserts (cold or warm) [*Craddock and Maxwell*, 1993; *Craddock et al.*, 1997; *Hynek and Phillips*, 2001; *Golombek and Bridges*, 2000]. This suggests either infrequent precipitation events, perhaps correlated with brief optimal periods associated with the pronounced quasi-cyclic climatic variation of Mars [*Laskar et al.*, 2004], or possibly associated with short optima associated with impacts producing craters in the 100 km+ diameter range [*Carr*, 1989; *Segura et al.*, 2002; *Colaprete et al.*, 2004]. We will discuss further the contrast between Noachian and the

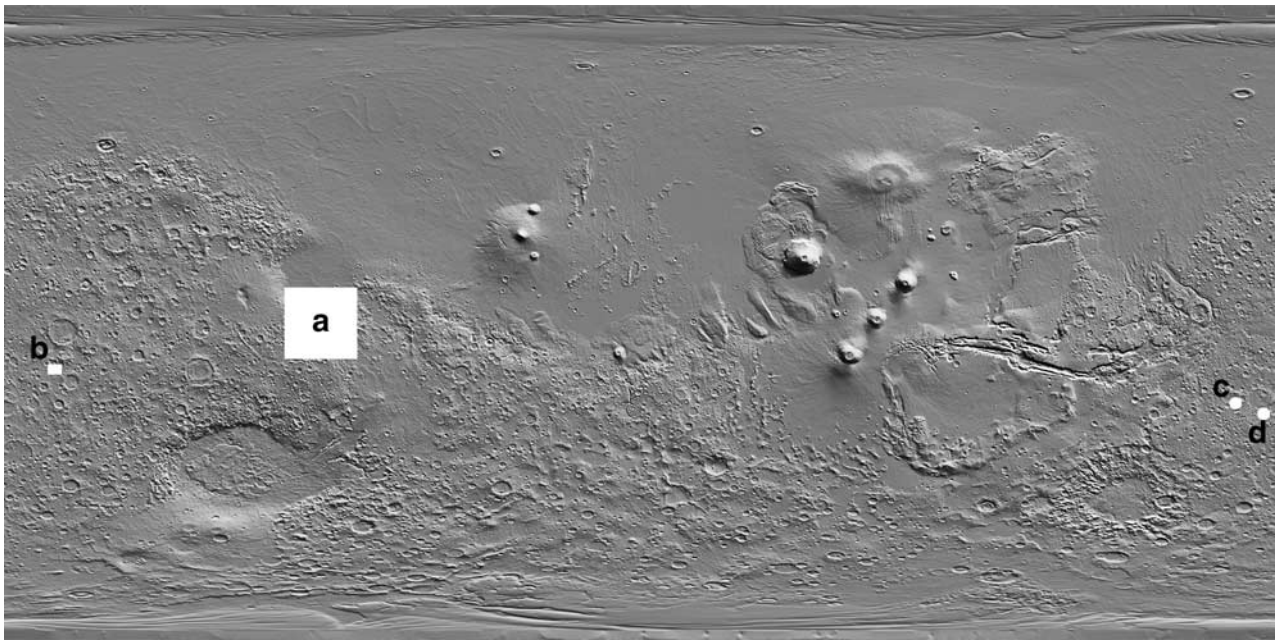

Figure 1. Shaded relief global map of Mars, extending from 0° to 360°E. Locations of the main study sites indicated as follows: a, Isidis rim (Figure 2); b, Evros Valles region (Figure 11); c, Parana Valles region (Figure 15); d, Pediment map region (Figure 16). Note that circles for locations c and d are not scaled to their corresponding figures.

late-stage erosional environment based upon observations presented below.

3. Late-Stage Fluvial Incision

[8] Relatively undegraded fluvial valleys are found widely in the equatorial highlands. Sparse, arroyo-like networks incise 50–350 m into what appear to be earlier Noachian fluvial basin deposits. We present observations from four channel systems in the Martian highlands: the southern Isidis basin margin, Evros Valles, Parana Valles, and a region in the Margaritifer Sinus highlands (Figure 1).

3.1. Isidis Basin Margin

[9] Integrated valley systems up to 800 km in length drain northward into the Isidis basin from its high-relief southern rim [*Crumpler and Tanaka*, 2003] (Figures 2 and 3). We examine below the geomorphic context of these valleys and quantify the patterns of valley incision.

3.1.1. Geomorphic Relationships

[10] In their downstream reaches these valleys are typically 2–4 km wide, with flat floors and valley walls approaching 30° in steepness (Figures 4 and 5). Except where they pass through deeper canyons where they traverse degraded rim remnants of the Isidis Basin (the Libya Montes), the valleys are typically sharply incised 50–350 m below relatively smooth intercrater plains surfaces. Both *Craddock and Howard* [2002] and *Crumpler and Tanaka* [2003] interpreted these plains to be Noachian sedimentary deposits shed from surrounding uplands. Figure 3a shows an elevation-cued interpretive map of the downstream portions of one of these valley systems (the "eastern valley" of *Crumpler and Tanaka* [2003]) showing the dissected basin deposits and contributing eroded highlands. Figure 3b presents an interpretive physiographic map of the region shown in Figure 3a. This map partially overlaps the area mapped by *Crumpler and Tanaka* [2003], and we identify in braces the units on their map that most closely correspond to our mapping. *Uplands* (brown) are high areas that are moderately fluvially dissected {Nm}. *Massifs* (red) are dissected mountains that comprise the Libya Montes {Nm}. *Dissected basin floors* (cyan) lie at the foot of uplands or massifs and appear to be generally planar surfaces that have been strongly fluvially dissected {NHf}. *Smooth basin floors* (blue) appear smooth at 100–200 m/pixel image resolution, although they may be rough at meter scale {Hi}. This unit occupies the lowest relative positions in the intercrater regions and may locally be entrenched by through-flowing drainage. *Smooth crater floors* (gray) comprise the interior of strongly degraded Noachian craters {Hi}. *Isidis basin deposits* (magenta) are mapped as an undifferentiated unit {Hk and Ht}. *Slightly degraded craters* (light green) have been only slightly modified by fluvial processes, and *postfluvial craters* (light green) were emplaced after the cessation of fluvial activity. The major *valley networks* (yellow lines) were dated as Lower to Upper Hesperian age on the basis of crater counts by *Crumpler and Tanaka* [2003] {Hd}. We include the incised channels within our late-stage features.

[11] In summary, by our interpretation the massifs and uplands of the southern highlands were extensively eroded during the Noachian, with sediment accumulating in intercrater basins and on crater floors. Some fraction of the eroded sediment was delivered to the Isidis basin floor. During the late-stage erosion the fluvial networks became integrated and valley incision dominated over deposition in the intercrater basins.

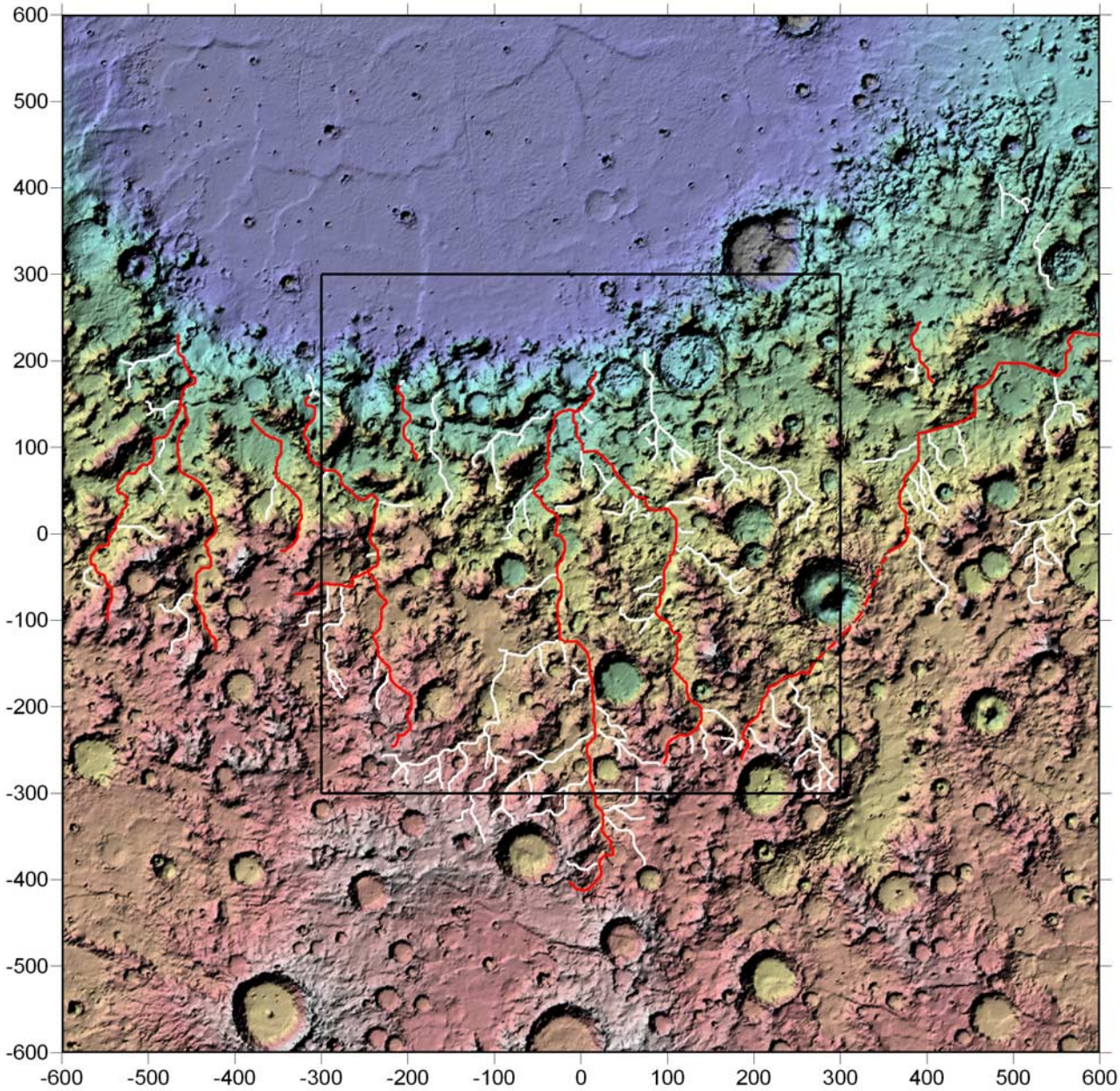

Figure 2. Shaded relief map of the southern rim of the Isidis basin. Map is centered on 90°E and 0°N, covering approximately 80° to 100°E and 10°S to 10°N. Axis labels are in kilometers relative to center of figure. Channel profiles were constructed for the drainage networks shown in white and red (e.g., Figure 9), with the red channels being used to quantify the amount of incision as a function of gradient (see Figure 10). Location of Figure 3 shown in black outline.

[12] Locally in the dissected and smooth basin floor units, the upper walls of craters and incised valleys exhibit layered sediments (e.g., Figure 6; also Figure 9 of *Crumpler and Tanaka* [2003]), supportive of a depositional origin for the basin deposits.

[13] The incised channels seldom extend headward onto crater walls or upland slopes, but they can extend far downstream, rejuvenating the Noachian drainage paths. Although *Baker and Partridge* [1986] described such valleys as ''pristine,'' MOC NA images show that they were modified by cratering, mass wasting, and eolian deposition, but to a lesser degree than the antecedent network (Figure 5). The incised valleys may gradually shallow and narrow until they merge imperceptibly into the undissected basin floors or upland surfaces. Locally, however, the valleys terminate abruptly in steep, amphitheater headwalls (Figure 7). Note that the incised valley shown in Figure 7 heads in an upland basin just outside the rim of a 75-km-diameter crater whose floor is about 1500 m below the amphitheater head of the incised valley.

[14] The upper walls of incised valleys and the intervalley surfaces of smooth and dissected basin floors often display an irregular surface texture with decameter-scale knobs and furrows, and, locally, a scabby texture (Figures 5, 8, and 13).

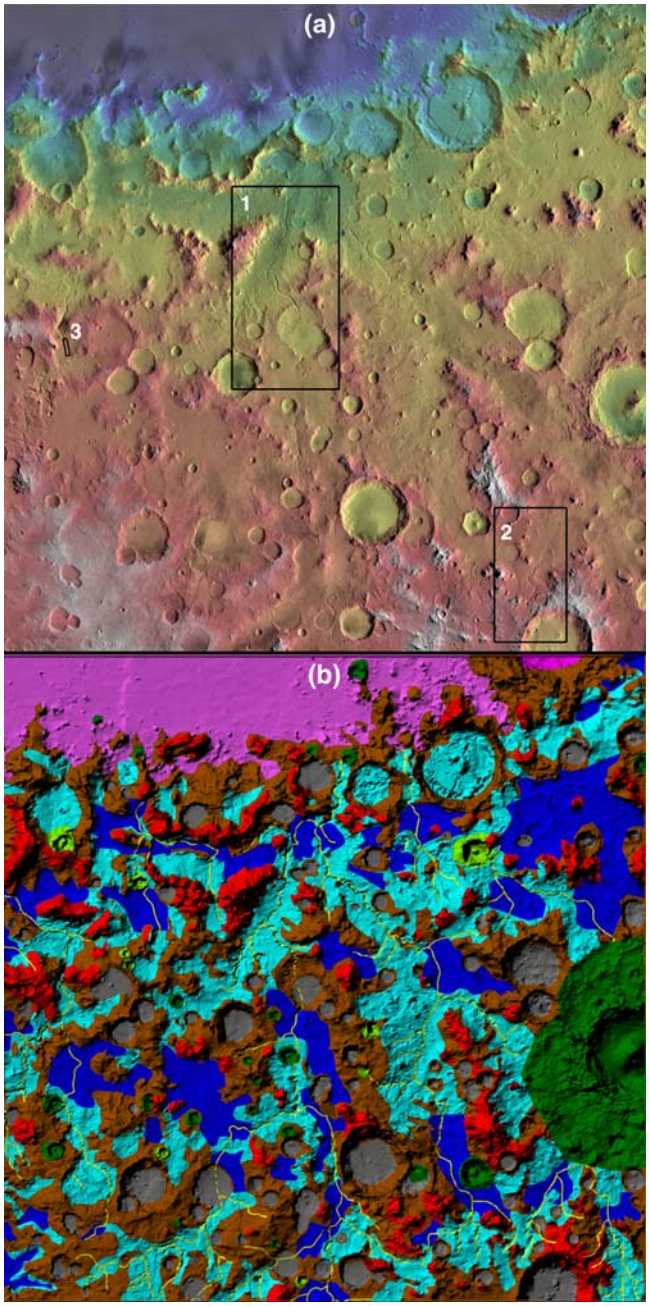

Figure 3. Landforms of the central southern Isidis Rim, centered on the "eastern valley" of *Crumpler and Tanaka* [2003]. (a) Elevation-cued image from the MDIM 2.1 Viking image mosaic. Image dimensions 600 × 600 km, centered on 90°E and 0°N. See Figure 2 for context. Box 1 shows location of Figure 4, box 2 is location of Figure 7, and box 3 is location of Figure 5. (b) Interpretive landform map on shaded-relief image from MOLA topography. Key: yellow, major valleys; magenta, Isidis basin deposits (undifferentiated); blue, smooth basin floor; cyan, dissected basin floors; brown, uplands; red, massifs; gray, smooth crater floors; dark green, postfluvial craters; light green, slightly degraded craters.

Where present, this textured surface often appears light-colored in MOC NA images. These same surfaces often appear bright in nighttime THEMIS IR images (Figures 4b, 7b, 12), indicating a high thermal inertia.

[15] Exposed channels within valleys are rare on Mars due to postformation eolian infilling and mass wasting. However, a THEMIS VIS image reveals an inner channel on the east branch of the "eastern valley" (Figure 8).

3.1.2. Valley Profiles and Valley Incision

[16] We investigated the longitudinal profiles and the spatial pattern of incision of the channels on the Isidis basin margin using MOLA data. The centerline of the major valley systems draining toward the northern lowlands (Figure 2) was digitized from the Viking Orbiter Mars Digital Image Mosaic (MDIM) 2.1 global image mosaics at about 3 km intervals, providing longitude and latitude pairs for each point. For each such point all MOLA PEDR (shot) observations within a specified search radius (3 km here) were utilized to determine the point with the lowest elevation, which is generally the valley floor. In addition, the maximum and average elevations within the search radius were recorded, as well as the 25th, 50th, and 75th percentile of elevations sorted from lowest to highest. If no MOLA observations fall within the search box, that digitized point

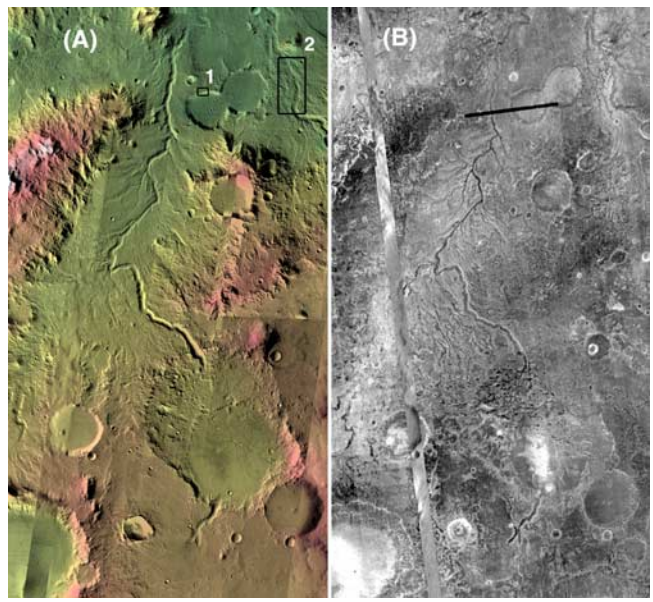

Figure 4. Incised channels and paleolake. (a) THEMIS daytime IR images overlain on MDIM 2.1 mosaic. Located at box 1 in Figure 2a. Image width 97.3 km. (b) THEMIS IR nighttime images of the same location. The valleys in the north end of the figure are interpreted to be incised into earlier alluvial basin deposits deposited at the foot of highlands bordering the basin (Figure 3b). Incised valley floors have low TI (dark in right image) due to eolian infilling, but upper rims and the dissected basin deposits are relatively bright, suggesting coarse sediment or indurated deposits. A double crater in the lower right has both entrance and exit breaches, suggesting that it was a paleolake. The valley system continues about 450 km upstream from the paleolake (Figure 9b). Box 1 shows location of Figure 6, and box 2 shows location of Figure 8.

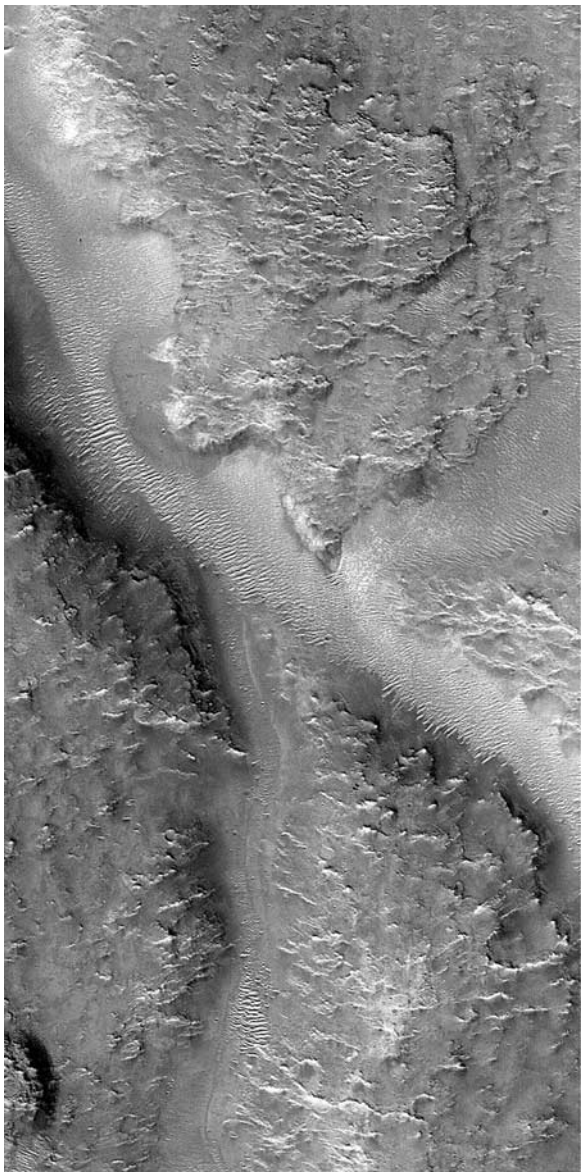

Figure 5. Incised valleys and basin deposits (MOC NA image R1002826). Image width 3.03 km. Located at box 3 in Figure 3a. Note the steep valley walls, the eolian valley infilling, and the rough, scabby texture of the intervalley surface.

is dropped from the database. Because the valleys are generally sharply incised below a comparatively planar surface, the 75th percentile elevation is assumed to closely correspond to the level of the surface into which the valley has incised. Figure 9a shows a profile of the lowest and 75th percentile elevations for the westernmost red channel in Figure 2. As can be seen the search procedure generally provides smooth valley and upland estimated profiles. This contrasts with construction of valley profiles from gridded data which results in more irregular profiles that are biased toward higher elevations because the gridding uses averages of MOLA observations. The use of the 75th percentile elevations diminishes the influence of local highs such as nearby crater rims in defining the upland surface.

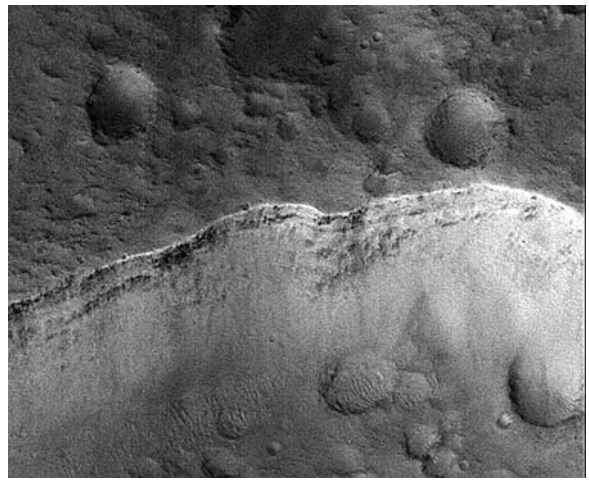

Figure 6. Layered deposits exposed in the upper wall of a crater (MOC NA image E0902318). Located at box 1 in Figure 4. Image width 3.11 km.

[17] Valley profiles as estimated by the MOLA shot data are generally smooth and downstream-sloping. The major artifacts from the present procedure occur where postincisional cratering occurred on or near the channel (e.g., Figure 9a), and occasional apparent local deformation by wrinkle ridges. This indicates that the Martian valley systems were well-integrated, although they are commonly stepped in the Isidis region, with locally steep

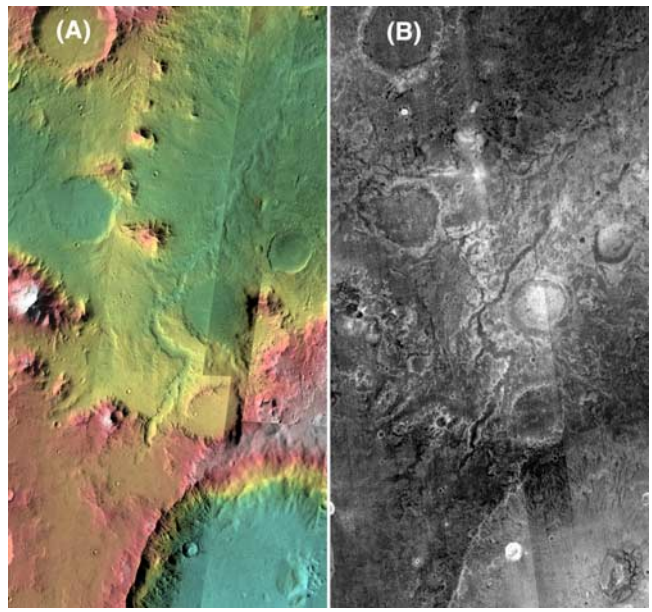

Figure 7. Incised valley. (a) THEMIS daytime IR images overlain on MDIM 2.1 mosaic. Located at box 2 in Figure 3a. Image width 79.7 km. (b) THEMIS IR nighttime images of the same location. Note that the amphitheater-like valley head extends nearly to the outer rim of the 70 km diameter crater whose floor is about 1500 m below the valley head. The valley margins and the dissected basin deposits in the upper right corner of the image are bright in the nighttime thermal IR, indicating high thermal inertia.

Figure 8. Inner channel within incised valley. Located at box 2 in Figure 4. A portion of THEMIS VIS image V03442003. Image width about 8.96 km.

reaches where the valleys pass through massif or upland ridges. An exception is the occurrence of a 180-m depression along the course of the valley profiled in Figure 9b at the location where the valley passes through the crater basin shown in Figure 4. This crater basin has both entrance and exit breaches, suggesting that the basin was at least occasionally occupied by an overflowing lake.

[18] From examination of a number of valley profiles it became apparent that the depth of incision below the upland surface was greater where the valley gradient was steepest. We quantified this by measuring valley gradient, apparent depth of incision, and channel length measured from the upstream limit of the incised valley network along 41 reaches in the Isidis basin rim (red lines in Figure 2). In selecting reaches we utilized only valley segments at least ten kilometers in length along which the valley profile had nearly constant gradient and depth of incision. We avoided sites where the valley incised through narrow ridges or where it was affected by postfluvial impacts. The relationship between apparent depth of incision, ΔZ, valley gradient, S, and cumulative downstream length, L, was determined by linear regression of the logarithms of the variables, yielding power function equations. The simplest relationship is between incision depth and valley gradient (Figure 10):

$$\Delta Z = 1452\, S^{0.48},\ R^2 = 0.60, \tag{1}$$

where R^2 is the fractional data variance explained by the regression and ΔZ is in meters. When downstream length is included,

$$\Delta Z = 993\, L^{0.15}\, S^{0.55},\ R^2 = 0.68, \tag{2}$$

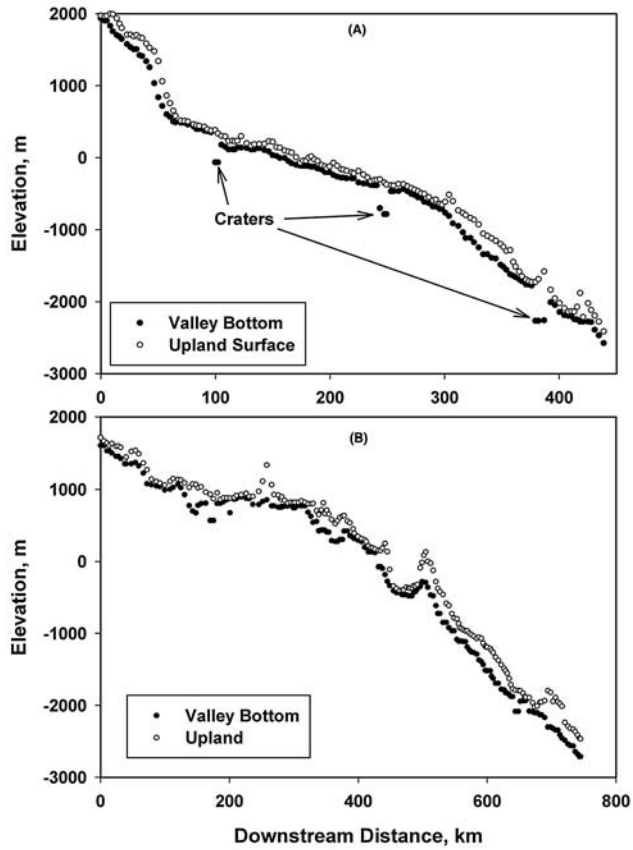

Figure 9. Representative profiles of valley systems in the Isidis region constructed from MOLA PEDR data. Valley bottoms are the lowest elevations recorded in the vicinity of the digitized location, and the upland surface is the 75th percentile (measured from the lowest local elevation) elevation within a 6 km search window. Profile a is along the westernmost red channel shown in Figure 2, and profile b is along the south-trending red valley in the center of Figure 2. Figure 4 shows about 200 km of this valley system between about downstream distance 400–600 km. Note the ~180 m depression within the presumed paleolake basin shown in Figure 4.

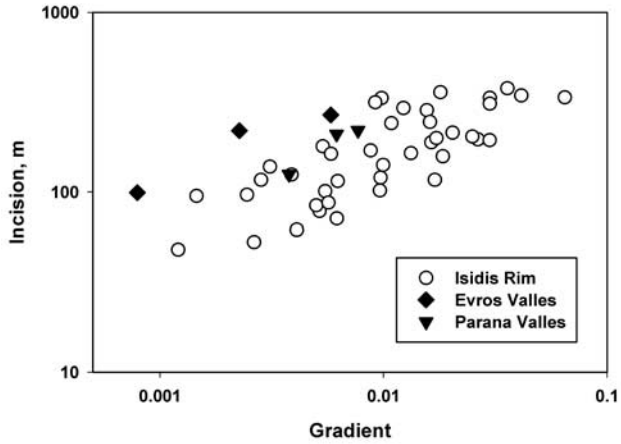

Figure 10. Relationship between the average depth of incision and valley gradient for segments of valleys 10 km or more in length. Locations of valleys in the Isidis Rim region included in the database are shown in Figure 2.

where L is in kilometers. The analysis thus confirms a positive relationship between incision depth, gradient, and cumulative downstream length.

3.2. Evros Valles

[19] The Evros Valles system south of the Schiaparelli basin drains westward from 20°E to 5°E at about 12°S. It lies at elevations from 0 to +1500 m. The main valley and major tributaries are incised 100–300 m into a broad basin surface graded to the center of the basin through which the valley flows (Figure 11). Faintly visible tributaries flow across the basin surface toward the main valley (Figure 11). These valleys are shallower, with gentler and less well-defined sidewalls than the incised master drainage, and they often join the incised valleys through profile convexities (knickpoints).

[20] As with the Isidis rim valleys, the upper valley walls appear bright in nighttime THEMIS IR, implying a high thermal inertia (Figure 12). These upper valley walls also have a rough, massive texture that appears bright in MOC NA images (Figure 13). The upper valley walls and fresh crater walls on the Evros basin locally display crude layering, suggesting the valleys have incised into sedimentary deposits (Figure 14).

[21] As with the Isidis basin valleys, the depth of incision along Evros Vallis correlates with profile gradient (Figure 10), although for a given gradient the depth of incision is greater than is typical for the Isidis basin valleys.

3.3. Margaritifer Sinus Region

[22] The Parana Valles system (Figure 15) also exhibits a branching valley system deeply entrenched below the level of a broadly sloping upland surface that forms the eastern rim of a ~330-km-diameter basin (the Parana Basin of *Grant and Parker* [2002]) between the Parana Valles system and its presumed continuation on the northwestward side of the basin as Loire Valles [*Grant*, 1987, 2000; *Grant and Parker*, 2002]. The origin of the upland surface is uncertain because it lacks highlands surrounding the basin which could have created a depositional platform. Strong Noachian denudation of this upland is suggested by the two highly degraded craters on the northeast side of Figure 15, the easternmost one of which has an outer rim that is highly eroded. Simulations by *Craddock and Howard* [2002] show that such upland "ghost" craters with flat floors can result from long-continued fluvial erosion of craters that form on local

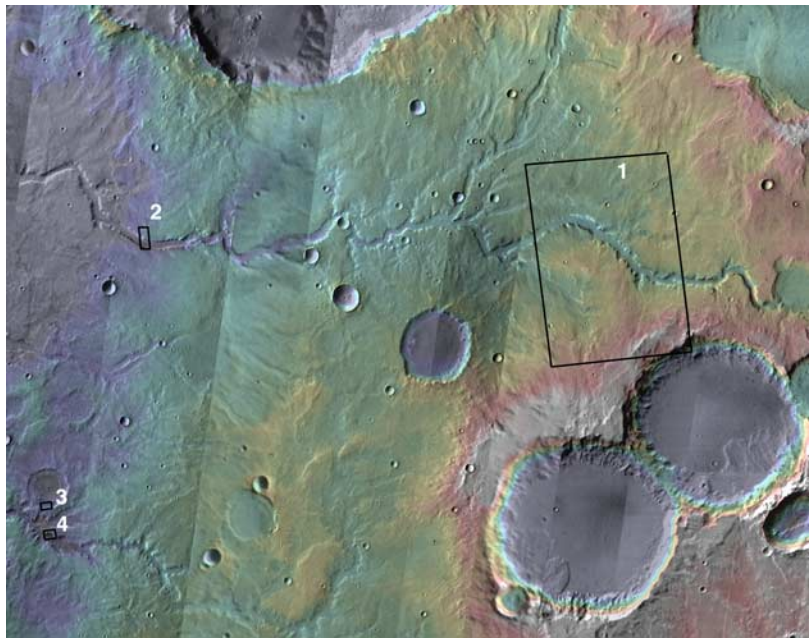

Figure 11. Evros Vallis overview. THEMIS daytime IR on MDIM 2.1 mosaic. Image centered at 14.51°E, 12.98°S. Image width 219 km. Box 1 shows location of Figure 12, box 2 shows location of Figure 13, and boxes 3 and 4 are Figures 14b and 14c.

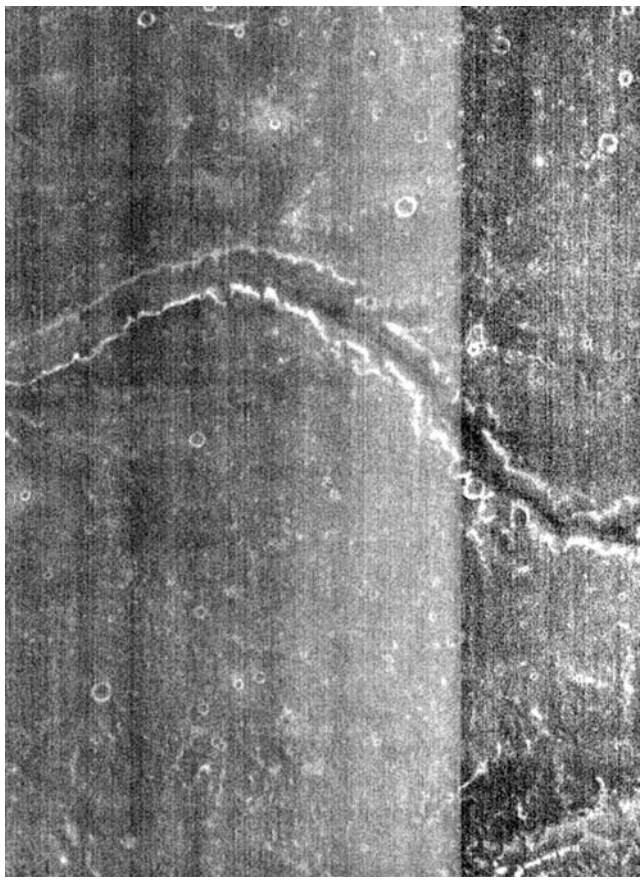

Figure 12. Nighttime THEMIS IR mosaic of Evros Valles. Located at box 1 in Figure 11. Image width 43.4 km.

highlands. The crater walls retreat, infilling the basin floor while external rim erosion creates deeply incised outer rims. The basin interior remains undissected until the outer wall has breached, which appears to have occurred on the westernmost of the two degraded craters just prior to the cessation of fluvial erosion. Thus the highly degraded craters suggest deep erosion of the upland surface, but the broad intervalley flats between the incised valleys are most consistent with localized late-stage valley incision into a relatively planar upland.

[23] As with the Isidis rim and Evros Valles system, the depth of valley incision correlates with downstream valley gradient (Figure 10), with incision depths consistent with averages for Isidis rim valleys.

[24] Another valley system in the Margaritifer Sinus region exhibits a suite of landforms that suggest a complicated erosional history (Figure 16). A broad ridge trending northwestward exhibits a radial drainage pattern which is segmented into concentric zones of similar degree of dissection bordered by downslope-facing scarps. These surfaces, described below, are most clearly expressed on the slope extending to the northeast from the ridge line. The highest zone is the narrow summit plateau mapped in red in Figure 16c. This ridge appears to be a remnant of a broad, sparsely dissected upland to the southeast of the mapped area which, during the Noachian, was being incised and backwasted by a series of northwestward-draining valleys, including the main drainages in Figure 16. This narrow plateau is bordered by a highly dissected sloping surface (blue in Figure 16c) which terminates downslope in a low scarp. Below this scarp lies a less dissected surface (green in Figure 16c) also bordered by a low scarp, below which is a broad, undissected valley floor (yellow) along the main drainageway.

[25] Interpretation: The spatial and vertical sequence of these surfaces, and the increasing degree of dissection with height suggest an evolutionary scenario involving alternating entrenchment and stability of the main drainageways. Erosion along the main drainageways initiated dissection of the highland surface (red). A period of relative stability of the main channels encouraged development of a low-relief pediment or alluvial fan surface leading from the edge of the retreating highland scarp to

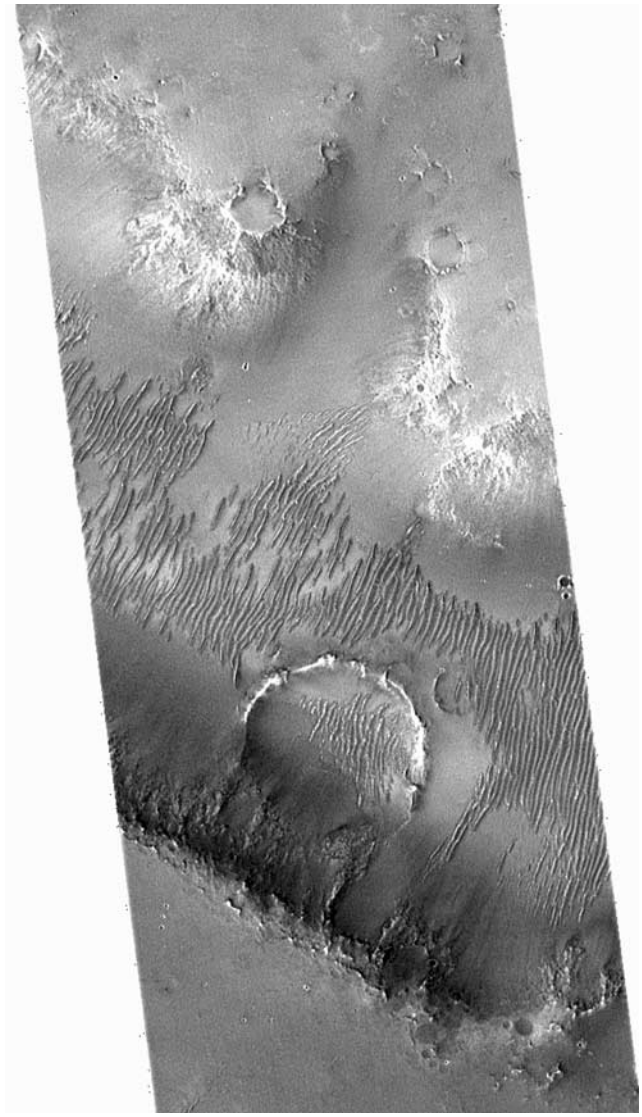

Figure 13. Detail of MOC NA image M1102194 of Evros Valles. Image width 2.18 km. Located at box 2 in Figure 11. Crater on valley floor is possibly exhumed, which would indicate sedimentary burial of the basin floor during the Noachian.

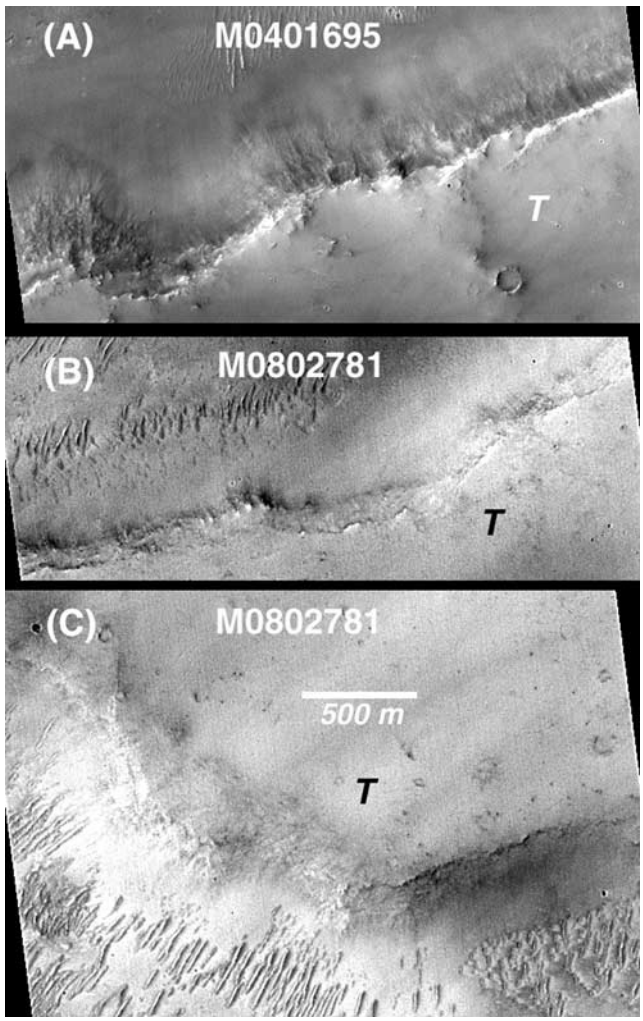

Figure 14. Exposed layering in the Evros Valles drainage basin in MOC NA images. Figures 14a and 14b show layering exposed in the walls of craters on the basin floor, and Figure 14c shows layering in the sidewall of a tributary to Evros Valles. Figure 14b is located at location 3 in Figure 11, and Figure 14c is at location 4. Figure 14a is downstream of Figure 11 at 9.4°E and 12.2°S. The plateau surfaces above the valley are labeled "T".

the main drainageway, probably in the general location of the present valley axis along the main valley (yellow). This was followed by an episode of entrenchment along the valley axis, initiating erosional dissection of the pediment/fan. Main valley incision again paused, allowing development of an erosional scarp moving headward into the earlier (blue) pediment surface coupled with formation of a new pediment/fan surface (green) graded to the valley axis. Finally, another pulse of erosion followed by stability caused incision below the green pediment/fan surface and development of a new surface (yellow) along the valley axis. Similar sets of pediments/fans of increasing age and dissection with distance from the master drainage occur in the Southwestern United States [*Bull*, 1991], particularly along the Rio Grande valley [*Ruhe*, 1967]. Episodes of valley erosion followed by stability or aggradation of drainageways can be caused either by headward migration of knickpoints or climatic oscillations affecting the balance of erosional sediment influx versus discharges through the fluvial system.

4. Alluvial Fans

[26] Large alluvial fans on the interior of a few 50+ km craters have been discovered in recent high-resolution images of the equatorial highlands [*Moore and Howard*, 2005]. These fans are 10 to 40 km in length and extend across the crater floors from intricately dissected alcoves eroded into the crater walls (e.g., Figure 17). These fans have gradients and morphometric relationships to their source basins that are similar to terrestrial counterparts. Probable remnants of distributary channels are often visible on the fan surfaces, radiating from the fan apex at the base of the source basins (Figure 17). Age dating of these fans from crater counts [*Moore and Howard*, 2005] places their origin to approximately the Noachian-Hesperian boundary, so that we consider below the possibility that they formed coevally with the incised valley systems. On terrestrial fans rainfall directly on the fans typically results in development of shallow valley networks on inactive portions of the fan. The Martian fans exhibit no on-fan drainage networks. The fans also usually lack fan-head trenches common on terrestrial fan systems and commonly associated with climatic transitions from Quaternary pluvial climates to more arid interglacials.

5. Deltas

[27] Recent high-resolution images have also revealed probable deltas within crater basins. The most definitive case occurs in the provisionally named Eberswalde crater at 326°E and 24°S [*Malin and Edgett*, 2003; *Moore et al.*, 2003; *Bhattacharya et al.*, 2005], where meandering

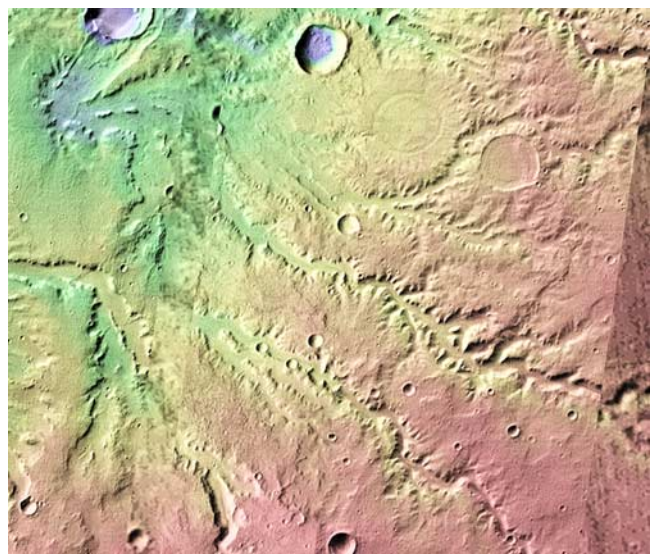

Figure 15. A portion of the Parana Valles. THEMIS IR mosaic on MDIM 2.1 mosaic. Image centered at 349.29°E, 22.72°S. Image width 78 km.

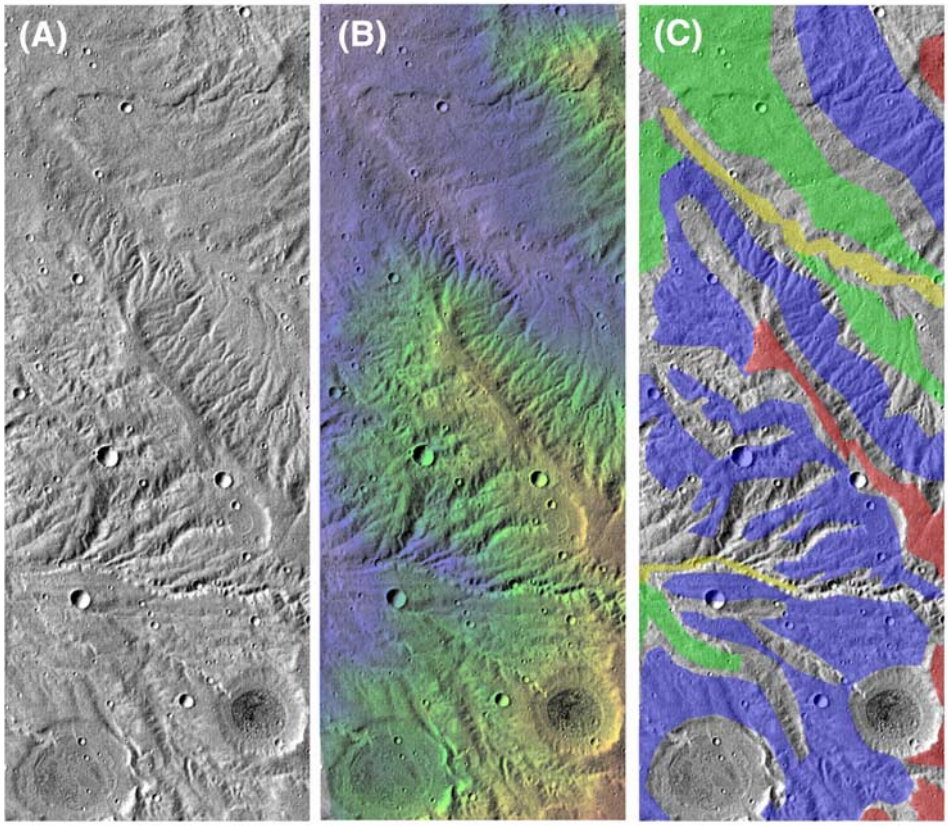

Figure 16. Pediments and fans in Margaritifer Sinus region. (a) THEMIS daytime IR image I01686001. (b) Image with elevation cueing. (c) Interpretation based upon landforms northeast of the central ridge (red) and speculatively extended elsewhere. Age sequence from oldest to youngest is red-blue-green-yellow (final drainage level). Image located at 357.02°E, 25.86°S. Image width 31 km.

distributary channels on the delta surface have been etched into positive relief by wind erosion. Other probable deltas have subsequently been identified in THEMIS or MOC images [*Irwin et al.*, 2004b, 2005c; *Fassett and Head*, 2005] and others were postulated on the basis of lower-resolution Viking Orbiter images [*Cabrol and Grin*, 1999; *Ori et al.*, 2000]. Figure 18 shows a probable delta in a crater northeast of the Hellas basin that radiates about nine kilometers onto the crater floor from the termination of a canyon. The contributing valley eroded through the crater rim, fed by a network of valleys draining a perched basin bordered by the rims of three nearby craters. Figure 19 shows a THEMIS VIS mosaic of the delta, which displays several fingers protruding beyond the main delta front that may have been small birdfoot distributaries. A few possible linear features that may be remnants of distributary channels occur on the delta surface, but they are poorly preserved. This delta, like the one in Eberswalde, has been differentially eroded resulting in inverted relief of channel deposits. The delta top slopes at about four degrees toward the center of the crater, and the marginal scarp (probable foreset beds) rises about 60 m from the crater floor. On the basis of topographic profiles from MOLA orbits crossing the delta, the volume of sediments is approximately 10.2 km^3. The canyon connecting the delta to the upland basin is about 240 m deep, and channels on the upper basin range from 10 to 100 m in depth. A crude estimate of the volume of the valley network feeding the delta based upon width, depth, and total length of the valleys visible in Figure 18 is 7.5 km^3. Thus it appears that the delta is primarily or wholly constructed of sediment eroded from the visible valley network, and that it formed coevally with the network. The gradient of the perched basin surface immediately above the canyon through the crater rim equals that of the delta top surface, which is also supportive of a coeval fluvial origin. A similar conclusion was reached for the Eberswalde crater delta and its upland valley network [*Moore et al.*, 2003].

[28] The craters that surround the upland basin, including the one containing the probable delta appear to be strongly degraded, with obliteration of ejecta and infilling of crater floors. The majority of this degradation must have occurred prior to the incision of the visible valley network and formation of the deltaic deposit.

6. Discussion: Implications for Martian Erosional History and Environments

[29] The suites of landform features that we discuss above appear to present a consistent pattern among widely distributed regions of the Martian equatorial cratered highlands. In the following discussion we present our interpretation of the sequence of events forming these

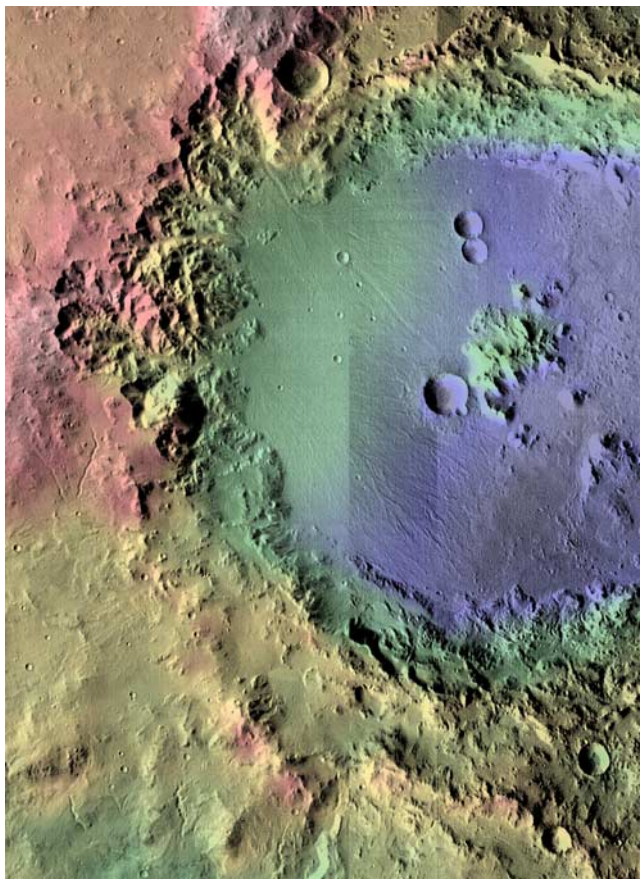

Figure 17. Fan complex North of the Hellas Basin. This is fan K of *Moore and Howard* [2005]. THEMIS daytime IR mosaic centered at 72.78°E, 21.81S. Image width 80.6 km.

features, the possible environmental controls producing them, and remaining issues and uncertainties.

6.1. Erosional and Depositional History

[30] The trunk channels of valley networks generally are sharply incised 50 to 350 m below relatively planar upland surfaces (Figures 3, 4, 7, 9, 11, and 15). Valley sidewalls are steep and generally show an abrupt scarp at the edge of the upland surfaces (Figures 5, 8, 13, and 20). The steep valley edges and deep incision prompted *Baker and Partridge* [1986] to label these as ''pristine'' valleys, although recent high-resolution images reveals that they have undergone significant postfluvial modification by eolian infilling, mass wasting, and impact cratering. We prefer the more neutral term ''incised valleys''. It is likely that most of the valley networks mapped from Viking images [e.g., *Pieri*, 1980; *Carr and Clow*, 1981; *Carr and Chuang*, 1997] represent incised valleys of the type discussed here.

[31] Most commonly the valleys dissect smooth-surfaced (at 100+ m scales) intercrater basins whose outer margins slope upward toward crater rims or eroded uplands (e.g., Figures 3 and 4). In some localities the upper walls of incised valleys and impact craters excavated into the basin surfaces exhibit crude layering (e.g., Figures 6 and 14). This suggests that the incised valleys dissect basins formed from sediment shed from adjacent uplands. The layering is less well defined than that of the intracrater deposits and regional blankets described by *Malin and Edgett* [2000b]. The fine-scale layering and ease of erosion of the latter deposits suggests fine-grained deposits of lacustrine or airfall origin, whereas the less distinct and less regular layering of the valley walls is consistent with coarser fluvial sedimentation. The pattern of basins dissected by the incised valleys suggests a temporal change from fluvial aggradation or planation of basin surfaces to a later epoch of incision.

[32] In some locations the pattern of incision appears to suggest a more varied history. The region shown in Figure 16 appears to have experienced alternating periods of formation of broad pediment or fan surfaces, presumably associated with stable or aggrading main channels, and incisional epochs, leading to fluvial dissection of the fans and pediments. Overall, however, these valley systems have undergone long-term incision and the areal extent of depositional pediments and valley bottoms appears to have been increasingly restricted toward the valley axis through time, whereas the earlier, broader pediment surfaces became increasingly dissected by fluvial erosion.

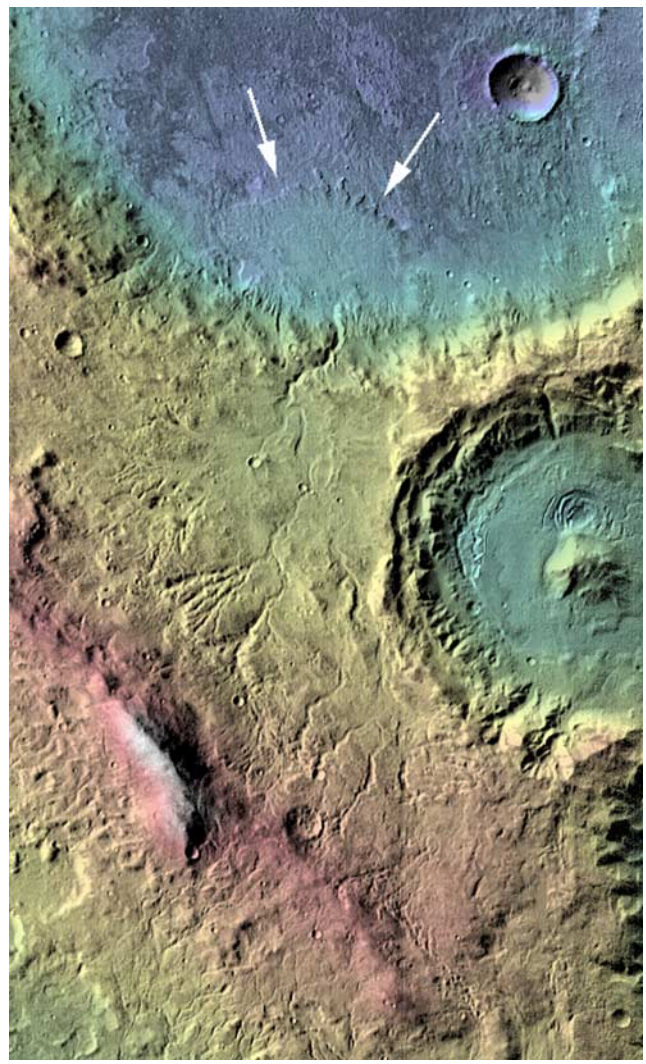

Figure 18. Delta and contributing basin NE of Hellas. THEMIS daytime IR. Arrows point to delta front. Mosaic centered at 83.03°E, 28.31°S. Image width 51.5 km.

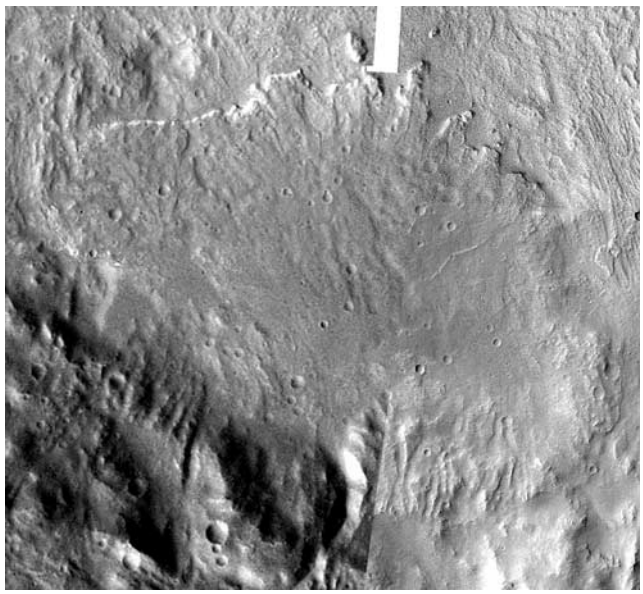

Figure 19. THEMIS VIS mosaic of delta shown in Figure 18. Image width 17.4 km.

[33] Where incised channel systems debouched into enclosed basins, such as at Eberswalde crater [*Malin and Edgett*, 2003; *Moore et al.*, 2003] and the basin shown in Figure 18, deltas were occasionally deposited [also see *Irwin et al.*, 2005b]. The equivalence of delta volumes to that of the feeding incised channel systems suggests that they formed coevally with the incised channels. The formation of deltas suggests sufficient duration of flows to create lakes.

[34] A number of large alluvial fans with runoff and sediment sources from steep, intricately dissected alcoves in crater walls have been identified on Mars [*Moore and Howard*, 2005] (Figure 17). Because their source basins are restricted to inner crater walls we cannot definitively link their origin to the same time period and same hydraulic regime as the incised channels and deltas. However, age dating based upon crater counting suggests an age in the same general time period of Martian history. The fans, like the deltas, imply appreciable, probably repeated flows extending over a time interval of many hundreds or thousands of years [*Moore et al.*, 2003; *Moore and Howard*, 2005]. Both the deltas and the fans share the important characteristic that the formative flows ceased abruptly, because the deltas were not dissected as a result of waning flows and lower lake levels [*Irwin et al.*, 2005b], and the fans likewise did not experience fan-head trenching or late-stage restriction of deposition to near the fan apex. Furthermore, the fans and deltas appear to lack examples of equivalent features formed earlier in Martian history. Although degraded Noachian craters have inward-sloping walls suggestive of alluvial deposition of sediment derived from erosion of crater rims [*Craddock and Howard*, 2002; *Forsberg-Taylor et al.*, 2004; *Moore and Howard*, 2005], the gradients of these surfaces are less than the large alluvial fans and they appear to have formed as bajadas from relatively uniform dissection of crater walls rather than localized incision of alcoves as in the case of the younger alluvial fans. Although numerous crater basins have inflowing valleys through crater wall breaches, obvious deltas are limited to where late-stage incised valleys occur upstream from the delta, and the delta volumes approximate the volume of the incised valleys. The similar age and depositional history suggest that both fans and deltas formed during the same time period on Mars. Notably, we have not been able to identify older, degraded alluvial fans or deltas of similar morphology to those discussed here within highland basins or craters. This suggests that the Noachian

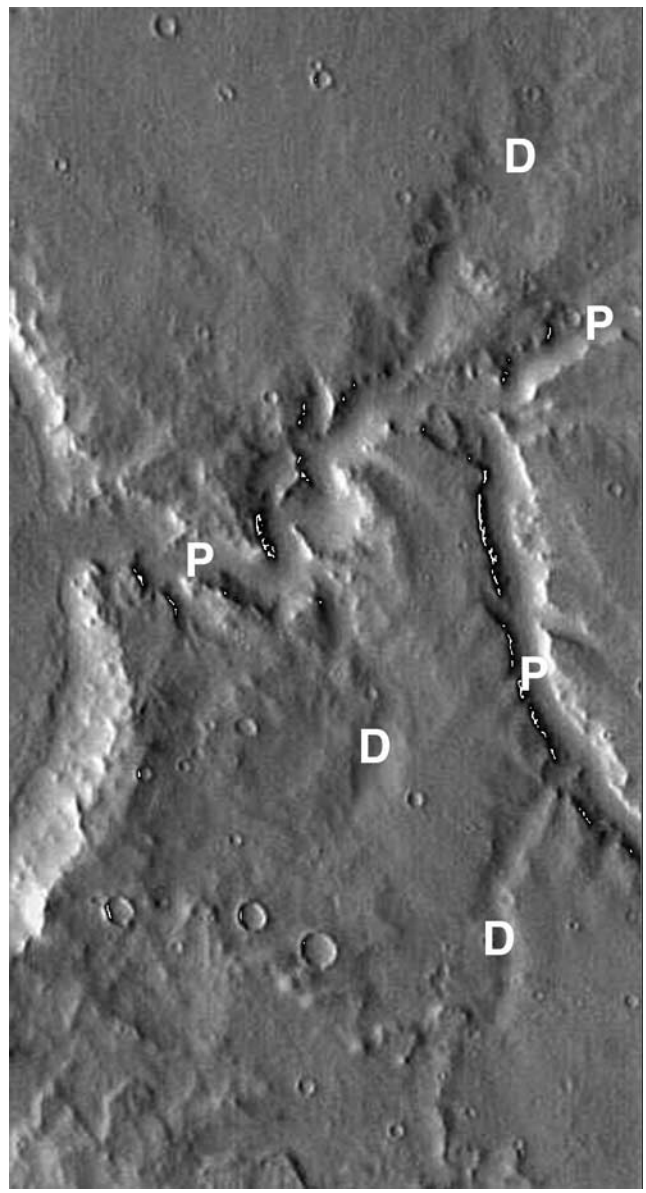

Figure 20. Incised valley breaching a crater rim. The probable cause of the incision is headward migration of knickpoint after breaching of the rim of the crater at the left of the image. THEMIS daytime IR image I01684010, centered at 29.5°E, 0.0°N. Image width 31 km. Deeply incised channels with sharp rims are labeled P, for "pristine," and shallow valleys with indistinct rims are labeled D, for "degraded." See text for further discussion.

erosional environment differed markedly from that forming the late-stage fluvial features.

6.1.1. Hydrologic Characteristics of Late-Stage Fluvial Activity

[35] The relative freshness of the late-stage fluvial features discussed here has permitted estimation of the magnitude of associated flows. *Moore et al.* [2003] utilized the width and meander wavelength of distributaries on the Eberswalde crater delta to estimate a formative discharge of approximately 700 m^3/s based upon scaling of terrestrial hydraulic geometry relationships to Martian gravity. *Jerolmack et al.* [2004] made a similar discharge estimate based upon a sedimentary model of fan/delta deposition. This discharge is approximately equivalent to the mean annual flood in terrestrial drainage networks of similar contributing area.

[36] Using similar hydraulic geometry scaling *Irwin et al.* [2005a] have utilized the width of inner channels in incised valleys to estimate discharges. They also estimated discharges of the same order of magnitude as mean annual floods in terrestrial drainage networks of similar contributing drainage area. The inner channel shown in the Isidis rim drainage in Figure 8 was not included in the *Irwin et al.* [2005a] database. The floor of the inner channel averages 183.6 m in width. *Irwin et al.* [2005a] utilize the scaled empirical relationship

$$Q = 1.4\,W^{1.22} \tag{3}$$

to estimate the channel-forming discharge, where discharge, Q, is in m^3/s and channel floor width, W, is in m. This provides an estimated discharge of 809 m^3/s. *Irwin et al.* [2005a] also use the estimated discharges and contributing drainage areas to develop a formative discharge – drainage area relationship for incised channels on the Martian highlands:

$$Q = 57\,A^{0.33}, \tag{4}$$

where drainage area, A, is in km^2. The inner channel in Figure 8 lies about 370 km downstream from its headwater source. Using a scaling relationship relating drainage area to mainstream length developed for terrestrial drainage networks ("Hack's Law" [*Hack*, 1957; *Rodriguez-Iturbe and Rinaldo*, 1997]):

$$L = 1.3\,A^{0.6}, \tag{5}$$

the indirectly estimated discharge from equations (4) and (5) is 1276 m^3/s. The more direct estimate from channel floor width is probably more accurate, but the estimate based upon drainage area suggests that the Isidis channel discharge is consistent with other highlands inner channels. The consistent relationship of discharge with contributing area, combined with the large magnitude of the discharges, strongly suggests flows through the valley networks were fed by precipitation, either directly from rainfall-runoff or indirectly from snowmelt, as suggested earlier by *Craddock and Howard* [2002].

[37] Whether the interior channels, such as that shown in Figure 8, have alluvial or bedrock banks is uncertain. If they are alluvial, the channel-forming flows would be equivalent to flows with recurrence interval of one to two years in terrestrial channels of equivalent size and contributing area. On the other hand, if the channel banks are bedrock, even larger channel-forming flows might have been necessary.

[38] These discharge estimates suggest appreciable discharges through the late-stage valley systems, but they leave uncertain the frequency and duration of such flows. If flows shared the recurrence interval characteristics of terrestrial drainage networks fed by precipitation, then the Eberswalde delta would have required thousands to tens of thousands of years to form [*Moore et al.*, 2003; *Bhattacharya et al.*, 2005]. By contrast, *Jerolmack et al.* [2004] suggest the overall flow period might have been only tens of years if flows were continuous rather than intermittent, and *Moore et al.* [2003] also acknowledge that the formation interval could be short if precipitation were caused by climatic change induced by a large impactor [*Segura et al.*, 2002].

6.1.2. Potential Causes of Valley Incision

[39] A pervasive pattern of late-stage valley incision occurs throughout the Martian cratered highlands within the trunk valleys. This incision contrasts with a dominance of local erosion of uplands and deposition within nearby basins earlier in the Noachian, with, apparently, less well-developed through-flowing drainage. A number of geologic and hydrologic controls could potentially cause valley incision. We evaluate possible causal conditions within the context of the observations and analyses presented above.

[40] River systems draining long regional slopes will gradually lower due to *long-term erosion* of the entire landscape. More or less spatially uniform downcutting of master drainage channels is documented in many terrestrial river systems. Such long-term erosion will not result in incised valleys unless either (1) the valley system is young and cutting into a previously uneroded surface or (2) environmental changes or tectonic deformation accelerate the erosional potential of the master streams relative to their smaller tributaries. The incised Martian valley systems appear to be superimposed upon a landscape created by extensive prior erosion (e.g., the Isidis rim region shown in Figures 2 to 8) so that an uneroded constructional surface is not apparent. Situations of this second type are discussed below.

[41] Over longer timescales most terrestrial fluvial systems undergo *gradual reduction of relief* within the entire drainage basin, which results in a diminishment in the quantity and coarseness of the sediment supply. Such landscapes, however, are characterized by minimal relief in the higher-order valleys and broad alluvial plains. Valley profiles are concave. Most Martian valley networks retain high relief, and high order valleys are incised rather than alluviated. Valley profiles are commonly irregular, with alternating steep and gentle reaches (Figure 9).

[42] Channels may incise due to *headward migration of knickpoints*. Knickpoints (locally steep reaches) commonly migrate headward through terrestrial valley systems. This downstream control of channel incision can occur due to, for example, local steepening of valleys by tectonic faulting or warping. Local incision of master valleys can also cause headward migration of knickpoints within

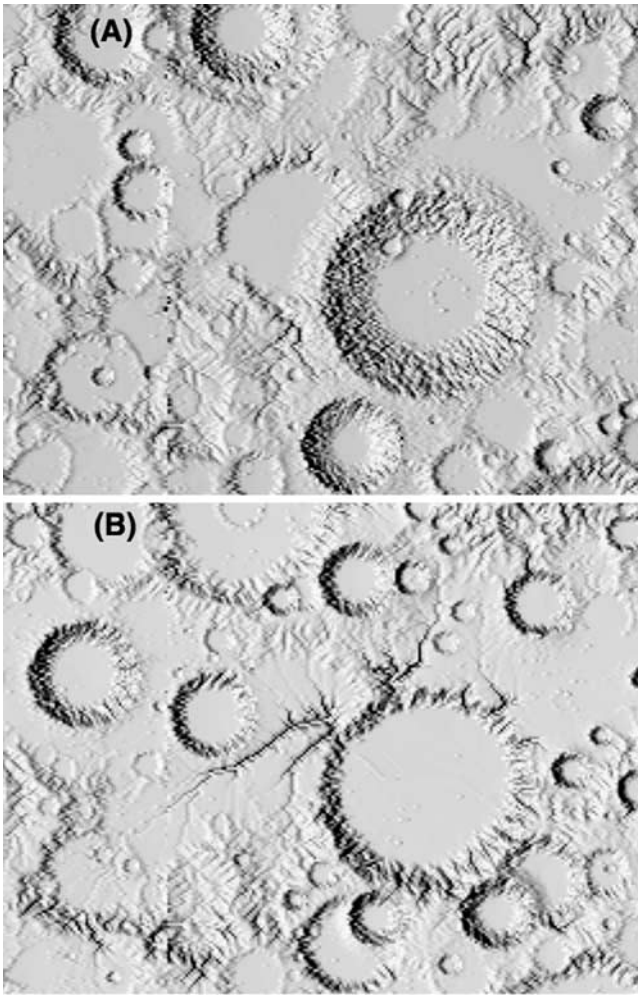

Figure 21. Simulated formation of incised channels due to entrance breaching of an impact crater. Details of the simulation model process formulation are presented by *Howard* [1994, 1997] and *Forsberg-Taylor et al.* [2004]. The simulated domain is about 100 km across. (a) A simulated fresh impact crater has formed in the right-center of the image within a relatively low elevation region. Note that random impacts and fluvial erosion have been occurring prior to this impact. (b) At a later stage the rim of the impact crater has been breached in several locations, resulting in formation of deeply incised valleys through headward migration of knickpoints. Breaching occurs both due to lowering of the crater rim by erosion occurring on the inner wall and due to continued infilling of the basin surrounding the crater by sediment deposited from erosion of surrounding uplands. In this simulation it is assumed that no runoff ponding occurs, so that breaching is not a consequence of lake overflow. Groundwater sapping is also not included as an erosional process. Note that additional impact craters have formed during the intervening time. The fluvial erosion is scaled to terrestrial semiarid environments, with about 200,000 simulated years occurring between Figures 21a and 21b.

tributaries. *Irwin et al.* [2004a], for example, conclude that rapid incision of Ma'adim Vallis due to paleolake overflow caused tributaries to be oversteepened at their junction with the stem valley (hanging valleys). This apparently caused headward migration of knickpoints through the tributary valley systems. Another potential cause of knickpoint formation and headward migration occurs when fluvial channels breach crater rims, creating a locally steep reach at the breach site that erodes headward. *Irwin and Howard* [2002] cite possible examples in Martian valley networks, and Figure 20 shows a likely example of a breached crater with an incised reach upstream, probably caused by headward migration of knickpoints. Simulation modeling of long-term erosion of cratered landscapes provides examples of headward incision driven by crater rim breaching (Figure 21). In this simulation rim breaching occurs as a joint result of erosional attack of the inner crater wall and infilling of the basin by sediment eroded from adjacent uplands. Although crater rim breaching, possible local faulting, and flood incision of master drainage might account for local cases of valley incision, they are unlikely to have caused the pervasive late-stage incision within the Martian cratered highlands. In particular, the drainage network shown in Figure 16 flows into a flat floored 360 km diameter basin, so that the base level for the valley system has either been stable or aggrading.

[43] *Baker and Partridge* [1986] and *Harrison and Grimm* [2005] suggest that incised ("pristine") valleys formed by headward migration of knickpoints driven by sapping erosion as groundwater emerged in the lower reaches of valley networks. According to this scenario, the groundwater outflow represents either the last stages of draining of aquifers that were recharged by precipitation during the Noachian or a hydrologic cycle driven by basal melting of snow and ice accumulated through precipitation [*Carr and Head*, 2003]. A number of observations cast doubt on the efficacy of groundwater flow to create the incised valley networks. The dimensions of inner channels and delta distributaries suggest formative discharges through late-stage valleys approximately equal to terrestrial channel-forming flows for equivalent contributing areas. Such discharges could only occur from effluent groundwater if permeability were very high, such as open-framework gravels. However, maintenance of such flows over a sufficient time to incise valley networks 50–350 m would require appreciable, areally distributed recharge through precipitation. Incised valleys occur at elevated locations with drainage basins (Figure 7) which are unlikely to be discharge locations for regional groundwater flow. In the situation shown in Figure 7 it would be most likely for regional groundwater flow to emerge at the floor of the nearby crater, some 1500 m below the level of the incised valley. Finally, depth of incision within valley networks shows a consistent relation to contributing area (parameterized by downstream distance) and valley gradient (equation (2)), which would be expected for basin-wide incision but unlikely for headwater migration of knickpoints.

[44] Valley incision can also occur because of *changes in the hydrologic regime and sediment supply.* In bedrock channel systems the rate of erosion depends upon flow

magnitude (see below), so that changes in flow regime could result in altered incision rates. In alluvial channel systems gradient depends functionally on the discharge regime, and the size and quantity of sediment supplied from the basin. In sand-bed channels, gradient increases with the sediment throughflow and decreases with increasing discharge. In gravel channels the balance is primarily between the size of supplied sediment and the discharge [e.g., *Howard*, 1980]. Thus incision might occur because of increased effective discharges or reduction in the size or quantity of supplied sediment.

[45] Valley incision due to a change in hydrologic regime or sediment supply is supported by the consistent relationship between the depth of incision, valley gradient, and position downstream within the drainage network (equation (2)). In fact, this relationship is consistent with models of bedrock channel incision in which the rate of downcutting, $\partial z/\partial t$, functionally depends upon some measure of the flow intensity, ϑ:

$$\frac{\partial z}{\partial t} = K(\vartheta - \vartheta_c), \tag{6}$$

where K is substrate erodibility and ϑ_c is a critical flow intensity required to initiate incision. For simulation of long-term channel incision the flow intensity is commonly parameterized as a power function of contributing drainage area, A, and local gradient, S, through the use of equations of hydraulic geometry [e.g., *Howard*, 1994, 1997; *Forsberg-Taylor et al.*, 2004]:

$$\frac{\partial z}{\partial t} = K(C\, A^m S^n - \vartheta_c), \tag{7}$$

where C is a constant. A functional dependence of erosion rates of this type has been observed in a number of terrestrial drainage basins, ranging from badlands to high-relief mountains [e.g., *Howard and Kerby*, 1983; *Stock and Montgomery*, 1999; *Tucker and Whipple*, 2002]. In particular, if the appropriate measure of flow intensity is assumed to be the mean shear stress exerted on the bed and discharge is assumed to be a power function (exponent e) of drainage area:

$$Q \propto A^e, \tag{8}$$

then the exponents take the values [*Howard*, 1994]:

$$m \approx 0.3e, \tag{9}$$

and

$$n = 0.7. \tag{10}$$

The observed exponent relating Martian incised valleys in equation (2) (0.55) is close to the gradient exponent, n, for a shear stress dependency. If equations (4), (5), and (9) are combined, the predicted exponent for shear stress dependency of incision rate on channel length equals 0.17, close to the 0.15 observed in equation (2).

[46] Many of the low-gradient valley segments utilized in the incision database are probably primarily alluvial channels. The rate of bed erosion in alluvial channels depends upon the spatial divergence of sediment flux (which can be expressed in terms of a spatial variation in shear stress) rather than the local value of shear stress, which is hypothesized to correlate with bedrock channel incision rates. The observation that Martian valley incision rates correlate with surrogate measures of shear stress (gradient and downstream length) suggests that erosion of the alluvial channel reaches is limited by the rate of incision into bedrock exposures within or immediately below the alluvial reaches.

[47] Incised valleys can also occur due to *erosion through layered bedrock*. An incised channel can result were a channel cuts through a resistant rock unit into a weaker underlying unit. This is a potential explanation for valleys such as Nirgal Valles, which cuts into Hesperian basalt flows, possibly having deepened and widened upon exposure of underlying weaker rocks. Exposure of weak layers in the highland bedrock stratigraphy, however, is unlikely to be a universal explanation for late-stage valley incision. The presence of rough-textured, apparently indurated material exposed in the upper walls of many incised valleys (e.g., Figures 5, 8, 13, and 14) raises the possibility that a resistant layer, presumably a duricrust, has hardened the surface layers of much of the cratered highlands. In terrestrial arid and semi-arid environments duricrusts sometimes develop sufficient strength and thickness to cause inverted topography during subsequent erosion [*Dixon*, 1994]. Weak duricrusts have been found at the Viking, Pathfinder, and MER lander sites, but they would not be of sufficient strength to affect erosion. Unfortunately, no landed mission has examined intact Noachian-age surfaces, so that direct confirmation is not possible at this time. The high thermal inertia of many upper incised canyon walls (e.g., Figures 4b, 7b, and 12) could be consistent with a resistant duricrust. More speculatively, the restriction of formation of large alluvial fans to localized sites on crater walls [*Moore and Howard*, 2005] (e.g., Figure 17) could result from erosion of alcoves only in locations where a duricrust has been breached. If such "case hardening" of the Noachian surface did occur, it would impose a critical shear stress (e.g., equation (7)) upon fluvial erosion and sediment transport that could restrict subsequent erosion only to downstream locations where sufficient water accumulates. It could also reduce sediment supply from headwaters, also tending to increase incision.

[48] In summary, the most likely explanations for the widespread late-stage incision of valley networks are a change in the hydrologic regime or sediment supply within the drainage basins, or possibly development and erosional breaching of a widespread duricrust layer. Possible environmental controls for such changes are discussed next.

6.1.3. Environmental Conditions During Late-Stage Fluvial Activity

[49] The observations cited above present a consistent picture of the late-stage fluvial activity in the equatorial Martian cratered highlands. During the late Noachian the highlands had been extensively eroded by fluvial processes, eroding inner and outer crater rims as well as Isidis rim massifs and steeper regional slopes (e.g., Figures 15 and 16), deeply filling crater interiors [*Craddock and Howard*, 2002; *Forsberg-Taylor et al.*, 2004] and creating broad

alluvial plains within intercrater basins. At about the Noachian-Hesperian transition (or possibly as late as mid-Hesperian) the major drainages incised into the earlier Noachian landscape, generally creating valleys 50–350 m deep in the intercrater basins. On the basis of the dimensions of delta distributaries and inner channels within incised valleys, fluvial flows during this time period were of a magnitude similar to channel-forming floods within terrestrial drainage networks for equivalent drainage areas. Flows at least episodically continued sufficiently long to flood craters along the valley axes up to several tens of kilometers in diameter, eroding both entrance and exit breaches through the crater walls (e.g., Figure 4). Where incised valleys entered craters, deltaic deposits were sometimes deposited. Probably during the same time period the walls of some deep craters were locally eroded into intricately dissected alcoves with the sediment being deposited as large alluvial fans on the crater floor (e.g., Figure 17). Equivalent types of fans and deltas seem not to have formed earlier in the Noachian. This period of fluvial activity appears to have ended abruptly, because fans and deltas were not entrenched by late-stage flows, and the last active inner channels within incised valleys record large flows.

[50] A number of environmental scenarios might have produced the observed fluvial features. In earlier discussion we have discounted scenarios involving a slow decay of the hydrological cycle resulting in less frequent or less intense flows. A change from runoff to sapping erosion likewise appears insufficient to provide the large discharges inferred from dimensions of fluvial channels formed during the late-stage incision. As discussed in section 6.1.3, channel incision could have resulted from a reduction of size or quantity of supplied sediment or from an increased magnitude of fluvial discharges. An increase in critical thresholds for erosion or sediment transport (e.g., equation (7)) could also focus erosion within larger channels. We suggest the following scenarios as possible candidates for the observed late-stage landform suite.

6.1.3.1. Increase in Global Temperature and in Precipitation Intensity

[51] Such a scenario might reduce the rate of physical weathering, and thus the amount and size of supplied sediment. Increase in precipitation intensity, although increasing both channel flows and sediment entrainment from slopes and low order channels, generally results in channel incision rather than aggradation. For example, *Howard and Kerby* [1983] noted that badland channels incise during the summer time period of intense thunderstorms and aggrade during the winter when rain intensity is lower and frost-induced mass wasting is greater. Such conditions might be triggered, for example, by greenhouse gasses introduced by a period of intense volcanism [*Phillips et al.*, 2001], by outflow floods spreading water across the northern lowlands [*Gulick and Baker*, 1989; *Baker et al.*, 1991; *Scott*, 1995; *Kreslavsky and Head*, 2002; *Fairen et al.*, 2003], by extreme excursions of obliquity [*Laskar et al.*, 2004], or by environmental effects of large impacts [e.g., *Carr*, 1989; *Segura et al.*, 2002].

6.1.3.2. Change From Rainfall-Runoff to Snowmelt Runoff

[52] Snowmelt-dominated fluvial systems tend to have hydrographs characterized by long flood peaks but relatively small sediment loads. Within the Colorado River system, for example, the bulk of sediment supplied to the river is delivered by local summer thunderstorms, but the largest discharges and most of the work of sediment transport and erosion are accomplished by early summer snowmelt, primarily deriving from the higher mountain ranges [*Howard and Dolan*, 1981]. In order to cause discharges sufficient to produce the observed dimensions of channels, melting of a snowpack would have had to be relatively rapid, for example, due to seasonal rather than obliquity climatic cycles, or due to some sudden, large-scale environmental perturbation. *Fassett and Head* [2004] suggest that snowmelt may have formed valley systems on Martian volcanoes. We do not think that the scenario of basal melting of a thick (hundreds of meters) snow/ice pack [*Carr and Head*, 2003] is a sufficient mechanism, both because of the high flow rates required and the occurrence of deltas and fans in basins, which are clearly subareal rather than sub-ice landforms.

6.1.3.3. Formation and Subsequent Erosion of a Regional Duricrust

[53] In this scenario a duricrust would develop on the Noachian landscape, perhaps gradually or during an episodic climate favoring its development, such as, perhaps, low intensity but frequent precipitation as snow or rain. A subsequent climate with higher intensity rainfall or rapid snowmelt would cause incision of major valleys within which flow rates would be sufficient to erode through the duricrust. A duricrust would also inhibit delivery of sediment to the channel system, leading to incision of alluvial streambeds.

[54] We have little evidence to choose among these scenarios at present, and combinations of the scenarios, or others we have not imagined, might have caused the late-stage features. In any case, conditions favorable to valley incision and formation of fans and deltas ceased rather abruptly sometime in the Hesperian on the equatorial cratered highlands.

6.2. Unresolved Issues

[55] We have presented observations and analyses that suggest a late-stage epoch of intense fluvial activity within the cratered highlands characterized by deep valley network incision and, locally, deposition of alluvial fans and deltas. We discuss here a number of issues that remain unresolved or poorly constrained.

[56] The timing of the late-stage fluvial activity relative to the established Martian chronology is uncertain within wide limits. The incised valleys, deltas, and fans occupy a small fraction of the total area of the highlands. What crater counts have been done [e.g., *Baker and Partridge*, 1986; *Crumpler and Tanaka*, 2003; *Moore and Howard*, 2005] yield large error limits but suggest ages from late Noachian to mid Hesperian. As a result, our evidence for synchronicity of valley network incision throughout the highlands and for equivalent ages for late-stage valley incision and for alluvial fan deposition remains circumstantial.

[57] The simplest scenario for late-stage fluvial activity would involve a single episode occurring throughout the highlands. The actual situation may have been more complex. For example, the multiple pediment surfaces in Figure 16 suggest episodes of alternating incision and

deposition, and stepped fan or delta deposits [*Irwin et al.*, 2005b] may likewise represent oscillating environmental conditions. Episodic erosional and depositional events in the highlands were suggested by *Grant and Schultz* [1990].

[58] The late-stage valley networks imply integrated flow through channel systems often exceeding several hundred kilometers in length (e.g., Figures 2 and 9) up to a maximum of more than 4,000 km [*Irwin et al.*, 2005b]. Yet valley profiles remain irregular and in some cases broadly convex (e.g., Figure 9). This irregularity and the lack of deeply incised canyons suggest that the mid to late Noachian epoch preceding the late-stage erosion was capable of extensive local redistribution of sediment (resulting, for example, in deeply filled basins and highly eroded craters (e.g., Figures 15 and 16), but that flows were ephemeral. The persistence of an unfilled crater 450 km downstream within a late-stage Isidis rim valley network (Figures 4 and 9) also suggests negligible long-distance sediment transport during the mid to late Noachian. The contrast between the hydrology of the late-stage valley networks and that during the Noachian are discussed more fully by *Irwin et al.* [2005b].

[59] Although a number of late-stage valley systems entering enclosed basins exhibit deltas or fan-deltas (e.g., Figure 17 and examples by *Malin and Edgett* [2003], *Moore et al.* [2003], and *Irwin et al.* [2005b]), many others do not, even though the basins may have both entrance and exit breaches (e.g., Figure 4). Because many of the valley systems entering these basins are large and experienced extensive late-stage entrenchment, sediment either was routed through the basins, or effective processes of sediment redistribution or removal must have occurred. Possible scenarios are discussed by *Irwin et al.* [2005b].

[60] The Isidis rim valley networks do not continue onto the floor of the Isidis basin. Incised valleys flowing toward the basin disappear at about −3000 m, although a few shallow sinuous channels extend lower. *Crumpler and Tanaka* [2003] suggest that the valleys transition to "terminal valley deposits" interpreted to be alluvial fans that extend outward to the basin floor at about −3800 m. However, obvious fluvial features such as the numerous distributaries seen on highlands fans and deltas [*Malin and Edgett*, 2003; *Moore et al.*, 2003; *Moore and Howard*, 2005] are lacking, although a few isolated, shallow sinuous channels extend across the terminal plains. Rather, this elevation zone has an unusual surface of low benches, ridges, depressions and splotchy textures that, as indicated by of their brightness in THEMIS nighttime IR images, have high thermal inertia. Only the slope below the termination of the westernmost valley in Figure 2 has a fan-like topographic form. The Isidis rim valleys clearly delivered appreciable sediment to the basin during late-stage erosion, however. A possible explanation for the paucity of fluvial depositional features is that fluvial flows interacted with standing water or ice deposits, or were later modified by ice or water within the basin.

[61] The validity and implications of the distinction made by *Baker and Partridge* [1986] between pristine and degraded channels remains uncertain. Pristine valleys are defined to be more deeply incised and to have steep, regular valley walls (e.g., "P" sites in Figure 20), whereas degraded valleys are shallower with more irregular walls ("D" in Figure 20). Similarly, the main channel and major tributaries of the Evros Valles system in Figure 11 are pristine, but the basin surface supports numerous barely distinguishable degraded valleys. As discussed earlier, "pristine" and "degraded" are somewhat inappropriate terms since all such valleys are heavily modified by later eolian, cratering, and mass wasting processes (e.g., Figures 5 and 13). A more important concern is whether the *Baker and Partridge* [1986] interpretation of a difference in formational age and process is valid. One possibility is that pristine versus degraded morphology merely reflects differential effects of postfluvial modification in valleys of differing initial depth and width, such that shallower valleys are more easily modified. A second possibility is that degraded valleys formed early in the late-stage fluvial incision of Noachian basins (the dissected basin floors of Figure 3b and the "fluvially modified terrain" of *Crumpler and Tanaka* [2003]), with later erosion (the incised valleys in Figure 3b) being restricted to major channels (yellow lines in Figure 3b). As discussed previously, we do not agree with the process distinction made by *Baker and Partridge* [1986] between runoff forming older degraded channels and subsequent groundwater sapping forming the pristine channels.

[62] The temporal relationship of the late-stage fluvial activity to other events occurring during its possible age range (late Noachian to mid Hesperian) remains uncertain, including outflow channel development, volcanic activity, mantling and glaciation in mid and high latitudes. If the age range can be narrowed, possible environments and causes of enhanced fluvial activity could be better evaluated.

7. Conclusions

[63] In this and a companion paper [*Irwin et al.*, 2005b] we present evidence that the final epoch of widespread fluvial erosion and deposition in the cratered highlands was characterized by integration of flow within drainage networks as long as 4000 km and trunk valley incision of 50 to 350 m into earlier Noachian depositional basins. Deltaic deposits formed locally where these incised valley systems debouched into enclosed basins. Large alluvial fans of sediment deposited from erosion of alcoves in steep crater walls probably formed contemporaneously with the late-stage erosion. The depth of incision below already established Noachian surfaces correlates strongly with the gradient and the total valley length, suggesting consistent regional hydrology. Discharge within the channel systems estimated by channel dimensions and scaling to terrestrial empirical relationships indicate flow rates equivalent to channel-forming floods in terrestrial drainage basins of equivalent size. Such high flow rates imply either runoff directly from precipitation or rapid melting of accumulated snow.

[64] This late-stage epoch of intense fluvial activity appears to be fundamentally different than the fluvial environment characteristic of most of the previous Noachian period. The late-stage epoch was characterized by incision of trunk valleys into basins that earlier had been sites of aggradation. We find no earlier Noachian equivalents of the large alluvial fans and deltas associated with the late-stage

fluvial activity. The earlier Noachian Period, however, was characterized by widespread fluvial erosion of highlands and crater rims, deeply infilling crater floors and intercrater basins. We speculate that the previous Noachian was characterized by a climate of ephemeral fluvial activity and local, rather than regional integration of drainage networks.

[65] The change in conditions that caused the enhanced late-stage fluvial erosion and deposition remains uncertain. One possibility is enhanced runoff volumes, either due to high rates of precipitation or to rapid melting of accumulated snowpacks. Another possibility is the development of a thick chemically indurated duricrust layer over much of the highlands, which would enhance runoff, reduce sediment yields, and focus erosion within larger channels.

[66] A number of issues remain uncertain concerning the late-stage fluvial activity, including the timing of the fluvial activity relative to Martian chronology (preliminary estimates place the late-stage activity within the range of late Noachian to mid-Hesperian) and the fate of sediment delivered from the highlands to the northern lowlands, including the possibility of interaction with oceans or ice covers. The relationship of the late-stage highland denudation to other activities such as outflow channel flooding, regional mantling episodes, formation of ice-related high-latitude features, and volcanic resurfacing remain uncertain. We do, however, find evidence that late-stage fluvial incision and deposition continued through the time period of fretted terrain development in the Aeolis Mensae region [*Irwin et al.*, 2004b; *Irwin et al.*, 2005b].

[67] We are continuing to investigate the late-stage fluvial activity through a number of means. The profiles and incision amounts of valley networks throughout the highlands are being digitized to expand the quantitative evaluation of incision amount and to look for regional differences. Hydrologic routing of runoff across the Martian highlands is being developed, including depression storage and evaporation. Spatial variations in modeled flow rates can be compared with differences in amounts of late-stage valley incision. The effects of duricrusts on patterns of erosion are being investigated using the DELIM simulation model [*Howard*, 1994, 1997; *Forsberg-Taylor et al.*, 2004]. We continue to search for diagnostic erosional and depositional features in high-resolution images and to narrow the geologic age of the late-stage activity through crater counting and regional geologic relationships.

[68] **Acknowledgments.** This research was supported by grants from NASA's Mars Data Analysis Program and the Planetary Geology and Geophysics Program. Helpful reviews were provided by Victor Baker and James Head III.

References

Arvidson, R. E., F. P. Seelos IV, K. S. Deal, W. C. Koeppen, N. O. Snider, J. M. Kieniewicz, B. M. Hynek, M. T. Mellon, and J. B. Garvin (2003), Mantled and exhumed terrains in Terra Meridiani, Mars, *J. Geophys. Res.*, *108*(E12), 8073, doi:10.1029/2002JE001982.

Baker, V. R., and J. B. Partridge (1986), Small Martian valleys: Pristine and degraded morphology, *J. Geophys. Res.*, *91*, 3561–3572.

Baker, V. R., R. G. Strom, V. C. Gulick, J. S. Kargel, G. Komatsu, and V. S. Kale (1991), Ancient oceans, ice sheets and the hydrological cycle on Mars, *Nature*, *352*(6336), 589–594.

Bhattacharya, J. P., T. H. D. Payenberg, S. C. Lang, and M. Bourke (2005), Dynamic river channels suggest a long-lived Noachian crater lake on Mars, *Geophys. Res. Lett.*, *32*, L10201, doi:10.1029/2005GL022747.

Bull, W. B. (1991), *Geomorphic Responses to Climatic Change*, 326 pp., Oxford Univ. Press, New York.

Burr, D. M., J. A. Grier, A. S. McEwen, and L. Keszthelyi (2002), Repeated aqueous flooding from the Cerberus Fossae: Evidence for a very recently extant, deep ground-water on Mars, *Icarus*, *159*, 53–73.

Cabrol, N. A., and E. A. Grin (1999), Distribution, classification, and ages of Martian impact crater lakes, *Icarus*, *142*, 160–172.

Carr, M. H. (1979), Formation of Martian flood features by release of water from confined aquifers, *J. Geophys. Res.*, *84*, 2995–3007.

Carr, M. H. (1989), Recharge of the early atmosphere of Mars by impact-induced release of CO_2, *Icarus*, *79*(2), 311–327.

Carr, M. H. (1996), *Water on Mars*, 229 pp., Oxford Univ. Press, New York.

Carr, M. H. (1999), Retention of an atmosphere on early Mars, *J. Geophys. Res.*, *104*, 21,897–21,910.

Carr, M. H., and F. C. Chuang (1997), Martian drainage densities, *J. Geophys. Res.*, *102*, 9145–9152.

Carr, M. H., and G. D. Clow (1981), Martian channels and valleys—Their characteristics, distribution, and age, *Icarus*, *48*, 91–117.

Carr, M. H., and J. W. Head III (2003), Basal melting of snow on early Mars: A possible origin of some valley networks, *Geophys. Res. Lett.*, *30*(24), 2245, doi:10.1029/2003GL018575.

Clifford, S. M. (1993), A model for the hydrologic and climatic behavior of water on Mars, *J. Geophys. Res.*, *98*(E6), 10,973–11,016.

Clifford, S. M., and T. J. Parker (2001), The evolution of the Martian hydrosphere: Implications for the fate of a primordial ocean and the current state of the Northern Plains, *Icarus*, *154*, 40–79.

Colaprete, A., R. M. Haberle, T. L. Segura, O. B. Toon, and K. Zahnle (2004), The effect of impacts on the early Martian climate, in *Second Conference on Early Mars*, Abstract 8016, Lunar and Planet. Inst., Houston, Tex.

Craddock, R. A., and A. D. Howard (2002), The case for rainfall on a warm, wet early Mars, *J. Geophys. Res.*, *107*(E11), 5111, doi:10.1029/2001JE001505.

Craddock, R. A., and T. A. Maxwell (1993), Geomorphic evolution of the Martian highlands through ancient fluvial processes, *J. Geophys. Res.*, *98*(E2), 3453–3468.

Craddock, R. A., T. A. Maxwell, and A. D. Howard (1997), Crater morphometry and modification in the Sinus Sabaeus and Margaritifer Sinus regions of Mars, *J. Geophys. Res.*, *102*, 13,321–13,340.

Crumpler, L. S., and K. L. Tanaka (2003), Geology and MER target site characteristics along the southern rim of Isidis Planitia, Mars, *J. Geophys. Res.*, *108*(E12), 8080, doi:10.1029/2002JE002040.

Dixon, J. C. (1994), Duricrusts, in *Geomorphology of Desert Environments*, edited by A. D. Abrahams and A. J. Parsons, pp. 82–105, CRC Press, Boca Raton, Fla.

Dohm, J. M., and K. L. Tanaka (1999), Geology of the Thaumasia region, Mars: Plateau development, valley origins, and magmatic evolution, *Planet. Space Sci.*, *47*, 411–431.

Fairen, A. G., J. M. Dohm, V. R. Baker, M. A. de Pablo, J. Ruiz, J. C. Ferris, and R. C. Anderson (2003), Episodic flood inundations of the northern plains of Mars, *Icarus*, *165*, 53–67.

Fanale, F. P., S. E. Postawko, J. B. Pollack, M. H. Carr, and R. O. Pepin (1992), Mars: Epochal climatic change and volatile history, in *Mars*, edited by H. H. Kieffer et al., pp. 1135–1179, Univ. of Ariz. Press, Tucson.

Fassett, C. I., and J. W. Head III (2004), Snowmelt and the formation of valley networks on Martian volcanoes, *Lunar Planet. Sci.*, *XXXV*, Abstract 1113.

Fassett, C. I., and J. W. Head III (2005), Fluvial sedimentary deposits on Mars: Ancient deltas in a crater lake in the Nili Fossae region, *Geophys. Res. Lett.*, *32*, L14201, doi:10.1029/2005GL023456.

Forsberg-Taylor, N. K., A. D. Howard, and R. A. Craddock (2004), Crater degradation in the Martian highlands: Morphometric analysis of the Sinus Sabaeus region and simulation modeling suggest fluvial processes, *J. Geophys. Res.*, *109*, E05002, doi:10.1029/2004JE002242.

Golombek, M. P., and N. T. Bridges (2000), Erosion rates on Mars and implications for climate change: Constraints from the Pathfinder landing site, *J. Geophys. Res.*, *105*, 1841–1854.

Grant, J. A. (1987), The geomorphic evolution of Eastern Margaritifer Sinus, Mars, in *Advances in Planetary Geology*, *NASA Tech. Memo., TM 89871*, pp. 1–268.

Grant, J. A. (2000), Valley formation in Margaritifer Sinus, Mars, by precipitation-recharged ground-water sapping, *Geology*, *28*(3), 223–226.

Grant, J. A., and P. H. Schultz (1990), Gradational epochs on Mars—Evidence from west-northwest of Isidis Basin and Electris, *Icarus*, *84*, 166–195.

Grant, J. A., and T. J. Parker (2002), Drainage evolution in the Margaritifer Sinus region, Mars, *J. Geophys. Res.*, *107*(E9), 5066, doi:10.1029/2001JE001678.

Gulick, V. C. (1998), Magmatic intrusions and a hydrothermal origin for fluvial valleys on Mars, *J. Geophys. Res.*, *103*, 19,365–19,388.
Gulick, V. C. (2001), Origin of the valley networks on Mars: A hydrological perspective, *Geomorphology*, *37*(3–4), 241–268.
Gulick, V. C., and V. R. Baker (1989), Fluvial valleys and Martian palaeoclimates, *Nature*, *341*, 514–516.
Gulick, V. C., and V. R. Baker (1990), Origin and evolution of valleys on Martian volcanoes, *J. Geophys. Res.*, *95*, 14,325–14,344.
Hack, J. T. (1957), Studies of longitudinal stream profiles in Virginia and Maryland, *U.S. Geol. Surv. Prof. Pap., P294-B*.
Harrison, K. P., and R. E. Grimm (2005), Evolution of Martian valley network formation: surface runoff to groundwater discharge, *Lunar Planet. Sci.*, *XXXVI*, Abstract 1218.
Hartmann, W. K. (2005), Martian cratering 8: Isochron refinement and the chronology of Mars, *Icarus*, *174*, 294–320.
Head, J. W., J. F. Mustard, M. A. Kreslavsky, R. E. Milliken, and D. R. Marchant (2003), Recent ice ages on Mars, *Nature*, *426*, 797–802, doi:10.1038/nature02114.
Howard, A. D. (1980), Thresholds in river regimes, in *Thresholds in Geomorphology*, edited by D. R. Coates and J. D. Vitek, pp. 227–258, Allen and Unwin, St Leonards, NSW, Australia.
Howard, A. D. (1994), A detachment-limited model of drainage-basin evolution, *Water Resour. Res.*, *30*(7), 2261–2285.
Howard, A. D. (1997), Badland morphology and evolution: Interpretation using a simulation model, *Earth Surf. Processes Landforms*, *22*(3), 211–227.
Howard, A., and R. Dolan (1981), Geomorphology of the Colorado River in the Grand Canyon, *J. Geol.*, *89*(3), 269–298.
Howard, A. D., and G. Kerby (1983), Channel changes in badlands, *Geol. Soc. Am. Bull.*, *94*(6), 739–752.
Hynek, B. M., and R. J. Phillips (2001), Evidence for extensive denudation of the Martian highlands, *Geology*, *29*(5), 407–410.
Hynek, B. M., and R. J. Phillips (2003), New data reveal mature, integrated drainage systems on Mars indicative of past precipitation, *Geology*, *31*(9), 757–760.
Irwin, R. P., III, and A. D. Howard (2002), Drainage basin evolution in Noachian Terra Cimmeria, Mars, *J. Geophys. Res.*, *107*(E7), 5056, doi:10.1029/2001JE001818.
Irwin, R. P., III, A. D. Howard, and T. A. Maxwell (2004a), Geomorphology of Ma'adim Vallis, Mars, and associated paleolake basins, *J. Geophys. Res.*, *109*, E12009, doi:10.1029/2004JE002287.
Irwin, R. P., III, T. R. Watters, A. D. Howard, and J. R. Zimbelman (2004b), Sedimentary resurfacing and fretted terrain development along the crustal dichotomy boundary, Aeolis Mensae, Mars, *J. Geophys. Res.*, *109*, E09011, doi:10.1029/2004JE002248.
Irwin, R. P., III, R. A. Craddock, and A. D. Howard (2005a), Interior channels in Martian valley networks: Discharge and runoff production, *Geology*, *33*(6), 489–492.
Irwin, R. P., III, T. A. Maxwell, A. D. Howard, R. A. Craddock, and J. M. Moore (2005b), An intense terminal epoch of widespread fluvial activity on early Mars: 2. Increased runoff and paleolake development, *J. Geophys. Res.*, doi:10.1029/2005JE002460, in press.
Irwin, R. P., III, T. A. Maxwell, A. D. Howard, R. A. Craddock, and J. M. Moore (2005c), A Noachian/Hesperian hiatus and erosive reactivation of Martian valley networks, *Lunar Planetary Sci.*, *XXXVI*, Abstract 2221.
Jerolmack, D. J., D. Mohrig, M. T. Zuber, and S. Byrne (2004), A minimum time for the formation of Holden Northeast fan, Mars, *Geophys. Res. Lett.*, *31*, L21701, doi:10.1029/2004GL021326.
Kreslavsky, M. A., and J. W. Head (2002), Fate of outflow channel effluents in the northern lowlands of Mars: The Vastitas Borealis Formation as a sublimation residue from frozen ponded bodies of water, *J. Geophys. Res.*, *107*(E12), 5121, doi:10.1029/2001JE001831.
Laskar, J., A. C. M. Correia, M. Gastineau, F. Joutel, B. Levrard, and P. Robutel (2004), Long term evolution and chaotic diffusion of the insolation quantities of Mars, *Icarus*, *170*, 343–364.
Malin, M. C., and K. S. Edgett (2000a), Evidence for recent groundwater seepage and surface runoff on Mars, *Science*, *288*, 2330–2335.
Malin, M. C., and K. S. Edgett (2000b), Sedimentary rocks of early Mars, *Science*, *290*, 1927–1937.
Malin, M. C., and K. S. Edgett (2003), Evidence for persistent flow and aqueous sedimentation on early Mars, *Science*, *302*, 1931–1934.
Mangold, N., C. Quantin, V. Ansan, C. Delacourt, and P. Allemand (2004), Evidence for precipitation on Mars from dendritic valleys in the Valles Marineris area, *Science*, *305*, 78–81.
Moore, J. M. (1990), Nature of the mantling deposit in the heavily cratered terrain of northeastern Arabia, Mars, *J. Geophys. Res.*, *95*, 14,279–14,289.
Moore, J. M., A. D. Howard, W. E. Dietrich, and P. M. Schenk (2003), Martian Layered Fluvial Deposits: Implications for Noachian Climate Scenarios, *Geophys. Res. Lett.*, *30*(24), 2292, doi:10.1029/2003GL019002.
Moore, J. M., and A. D. Howard (2005), Large alluvial fans on Mars, *J. Geophys. Res.*, *110*, E04005, doi:10.1029/2004JE002352.
Mouginis-Mark, P. (1990), Recent water releases in the Tharsis region of Mars, *Icarus*, *84*, 362–373.
Ori, G. G., L. Marinangeli, and A. Baliva (2000), Terraces and Gilbert-type deltas in crater lakes in Ismenius Lacus and Memnonia (Mars), *J. Geophys. Res.*, *105*(E7), 17,629–17,641.
Phillips, P. J., et al. (2001), Ancient geodynamics and global-scale hydrology on Mars, *Science*, *291*(5513), 2587–2591.
Pieri, D. C. (1980), Martian channels: Distribution of small channels in the Martian surface, *Icarus*, *27*, 25–50.
Rodriguez-Iturbe, I., and A. Rinaldo (1997), *Fractal River Basins: Chance and Self-Organization*, 547 pp., Cambridge Univ. Press, New York.
Ruhe, R. V. (1967), Geomorphic surfaces and surficial deposits in southern New Mexico, *Mem. N. M. Bur. Mines Miner. Resour.*, *18*, 66 pp.
Scott, D. H. (1995), Map of Mars showing channels and possible paleolake basins, *U.S. Geol. Surv. Misc. Invest. Ser., Map I-2461*.
Segura, T. L., O. B. Toon, A. Colaprete, and K. Zahnle (2002), Environmental effects of large impacts on Mars, *Science*, *298*(5600), 1977–1980.
Soderblom, L. A., T. J. Kreidler, and H. Masursky (1973), Latitudinal distribution of a debris mantle on the Martian surface, *J. Geophys. Res.*, *78*(20), 4117–4122.
Stepinski, T. F., and M. L. Collier (2004), Extraction of Martian valley networks from digital topography, *J. Geophys. Res.*, *109*, E11005, doi:10.1029/2004JE002269.
Stock, J. D., and D. R. Montgomery (1999), Geologic constraints on bedrock river incision using the stream power law, *J. Geophys. Res.*, *104*(B3), 4983–4993.
Tanaka, K. L. (1986), The stratigraphy of Mars, *Proc. Lunar Planet. Sci. Conf. 17th*, Part 1, *J. Geophys. Res.*, *91*, suppl., E139–E158.
Tanaka, K. L. (1999), Debris-flow origin for the Simud/Tiu deposit on Mars, *J. Geophys. Res.*, *104*, 8637–8652.
Tucker, G. E., and K. X. Whipple (2002), Topographic outcomes predicted by stream erosion models: Sensitivity analysis and intermodel comparison, *J. Geophys. Res.*, *107*(B9), 2179, doi:10.1029/2001JB000162.

A. D. Howard, Department of Environmental Sciences, University of Virginia, P.O. Box 400123, Charlottesville, VA 22904-4123, USA. (ah6p@virginia.edu)
R. P. Irwin III, Center for Earth and Planetary Studies, National Air and Space Museum, Smithsonian Institution, 6th Street and Independence Avenue SW, Washington, DC 20013-7012, USA. (irwinr@si.edu)
J. M. Moore, NASA Ames Research Center, MS 245-3, Moffett Field, CA 94035, USA. (jeff.moore@nasa.gov)